

INFORMATION TO USERS

The most advanced technology has been used to photograph and reproduce this manuscript from the microfilm master. UMI films the text directly from the original or copy submitted. Thus, some thesis and dissertation copies are in typewriter face, while others may be from any type of computer printer.

The quality of this reproduction is dependent upon the quality of the copy submitted. Broken or indistinct print, colored or poor quality illustrations and photographs, print bleedthrough, substandard margins, and improper alignment can adversely affect reproduction.

In the unlikely event that the author did not send UMI a complete manuscript and there are missing pages, these will be noted. Also, if unauthorized copyright material had to be removed, a note will indicate the deletion.

Oversize materials (e.g., maps, drawings, charts) are reproduced by sectioning the original, beginning at the upper left-hand corner and continuing from left to right in equal sections with small overlaps. Each original is also photographed in one exposure and is included in reduced form at the back of the book. These are also available as one exposure on a standard 35mm slide or as a 17" x 23" black and white photographic print for an additional charge.

Photographs included in the original manuscript have been reproduced xerographically in this copy. Higher quality 6" x 9" black and white photographic prints are available for any photographs or illustrations appearing in this copy for an additional charge. Contact UMI directly to order.

U·M·I

University Microfilms International
A Bell & Howell Information Company
300 North Zeeb Road, Ann Arbor, MI 48106-1346 USA
313/761-4700 800/521-0600

Order Number 1830839

Fermi energy levels of fine calcites prepared in different ways

Han, Young H., M.S.

University of Nevada, Reno, 1989

U·M·I

300 N Zeeb Rd.
Ann Arbor, MI 48106

University of Nevada

Reno

Fermi Energy Levels of Fine Calcites

Prepared in Different Ways

A thesis submitted in partial fulfillment of the
requirements for the degree of Master of Science
in Metallurgical Engineering

by

Young H. Han

July 1988

The thesis of Young H. Han is approved :

Ross W Smith
Thesis Adviser

Ross W Smith
Department Chairman

Ann Forsyth
Dean, Graduate School

University of Nevada

Reno

August 1988

ACKNOWLEDGEMENT

The author thanks Dr. R. W. Smith (thesis advisor) for his constant supervision and encouragement in the course of this project as well as to Dr. R. Reddy and Dr. N. Salibi for their criticism and advice. The author is indebted to Dr. B. Johnson for his help in solving technical problems. Grateful acknowledgement is made to Mineral Industry Waste Treatment and Recovery Generic Centers, University of Nevada-Reno, for financial support.

TABLE OF CONTENTS

SECT.	PAGE
ACKNOWLEDGEMENTS.....	i
CONTENTS.....	ii
LIST OF FIGURES AND TABLE.....	iii
ABSTRACT.....	iv
I. INTRODUCTION.....	1
II. THEORY.....	7
III. EXPERIMENTAL PROCEDURE.....	20
Sample Preparation.....	20
Sample Holder.....	22
IV. RESULTS AND DISCUSSION.....	26
V. CONCLUSION.....	45

VI. SUMMARY..... 54

REFERENCES..... 55

APPENDIX..... 59

I. DISCUSSION OF INTRINSIC CONDUCTIVITY

II. THERMOELECTRIC POWER

III. DATA OF THERMOELECTRIC POWER AND FERMI LEVEL

**(ICELAND SPAR, ALBASPHERE, ALBACAR, ULTRAFINE,
ALBAGLOS, VICRON, MISSISSIPPI LINE)**

LIST OF FIGURES AND TABLE

FIGURE 1. DISLOCATIONS. (A) SHEAR DISLOCATION (B) SCREW DISLOCATION (C) EDGE DISLOCATION

FIGURE 2. POINT DEFECTS. (A) VACANCY (B) INTERSTITIAL (C) DISPLACEMENT TO THE INTERSTITIAL SITE (D) DISPLACEMENT TO SURFACE

FIGURE 3. ELECTRON ENERGY BAND LEVELS FOR METALS WITH PARTLY FILLED CONDUCTION BAND, INTRINSIC SEMICONDUCTORS WITH A NARROW BAND GAP, AND INSULATORS WITH A HIGH VALUE FOR E_g .

FIGURE 4. (A) SURFACE STRUCTURE OF CALCITE (1011), (B) CRYSTAL STRUCTURE OF CALCITE.

FIGURE 5. (A) FERMI DISTRIBUTION (INTRINSIC SEMICONDUCTOR). SINCE AN INTRINSIC SEMICONDUCTOR HAS AS MANY HOLES AS CONDUCTION ELECTRONS. (B) THE HOLE, 0 , MOVES TOWARD THE NEGATIVE ELECTRODES AS IF IT WERE A POSITIVE CHARGE.

FIGURE 6. SAMPLE AND SAMPLE HOLDER.

FIGURE 7. SIDE VIEW OF THE FURNACE USED.

FIGURE 8. TO 14. ELECTRICAL CONDUCTIVITY VERSUS RECIPROCAL TEMPERATURE FOR ICELAND SPAR, ALBASPHERE, ALBACAR, ULTRAFINE, ALBAGLOS, VICRON, MISSISSIPPI LIME.

FIGURE 15. ELECTRICAL CONDUCTIVITY VERSUS RECIPROCAL ABSOLUTE TEMPERATURE FOR CALCITE BY CARTA, M. ET AL..

FIGURE 16. TO 22. CHARGE CARRIER CONCENTRATION FOR ICELAND SPAR, ALBASPHERE, ALBACAR, ULTRAFINE, ALBAGLOS, VICRON, MISSISSIPPI LIME.

FIGURE 23. POSITION OF FERMI LEVEL AS A FUNCTION OF TEMPERATURE FOR CALCITE BY CARTA, M. ET AL..

FIGURE 24. TO 30. POSITION OF FERMI LEVEL AS A FUNCTION OF TEMPERATURE FOR ICELAND SPAR, ALBASPHERE, ALBACAR, ULTRAFINE, ALBAGLOS, VICRON, MISSISSIPPI LIME.

TABLE 1. CHARACTERISTICS OF CALCIUM CARBONATES STUDIED.

FIGURE 7. SIDE VIEW OF THE FURNACE USED.

FIGURE 8. TO 14. ELECTRICAL CONDUCTIVITY VERSUS RECIPROCAL TEMPERATURE FOR ICELAND SPAR, ALBASPHERE, ALBACAR, ULTRAFINE, ALBAGLOS, VICRON, MISSISSIPPI LIME.

FIGURE 15. ELECTRICAL CONDUCTIVITY VERSUS RECIPROCAL ABSOLUTE TEMPERATURE FOR CALCITE BY CARTA, M. ET AL..

FIGURE 16. TO 22. CHARGE CARRIER CONCENTRATION FOR ICELAND SPAR, ALBASPHERE, ALBACAR, ULTRAFINE, ALBAGLOS, VICRON, MISSISSIPPI LIME.

FIGURE 23. POSITION OF FERMI LEVEL AS A FUNCTION OF TEMPERATURE FOR CALCITE BY CARTA, M. ET AL..

FIGURE 24. TO 30. POSITION OF FERMI LEVEL AS A FUNCTION OF TEMPERATURE FOR ICELAND SPAR, ALBASPHERE, ALBACAR, ULTRAFINE, ALBAGLOS, VICRON, MISSISSIPPI LIME.

TABLE 1. CHARACTERISTICS OF CALCIUM CARBONATES STUDIED.

SECTION I
INTRODUCTION

This work presents an experimental investigation of the measurement of the Fermi level of various calcium carbonates. It was performed in order to determine whether there were differences in the Fermi level of calcium carbonates which were prepared in different ways. For the measurement of Fermi level the conductivity and the thermoelectric power (Seebeck coefficient) of the each sample were measured and calculated and the variation of the charge carrier concentrations in relation to temperature for various calcium carbonates was calculated. Measurements were made as a function of the temperature ($250^{\circ}\text{K} - 600^{\circ}\text{K}$) and performed in an inert atmosphere (argon gas).

Natural calcites are usually "n" type semiconductors. Various treatments such as heating or manner of grinding the material can change the electrophysical character of the mineral. The adsorption of ionic substances should be directly affected by such electrophysical properties and thus affected by method of pretreatment such as grinding. Several kinds of calcites were studied and the Fermi level of each sample measured and compared.

In the field of mineral dressing the first reported research developed on the basis of the solid - state physics dates back only to relatively recent years. Since then, much work has been carried out, notably in conductance electric separation [1,2,6], triboelectric separation [2,7-10], and flotation [2,6,11,12]. The position of the Fermi level determines the charge transfer direction across the interface of two solid phases and thus can affect such separation processes.

Kay interruption in the strict periodic pattern of the crystal lattice of minerals (various types of impurity and lattice defects in the bulk and the sharp break of the crystal lattice at the surface [13,14]) causes deviation from the ideal energy structure of solids and constitutes the starting point of energy exchange. The larger the displacement from equilibrium conditions between the mineral surface and phase in contact, the more important are the energy changes. These exchanges consist principally of electron transfer from one phase to the other in electric separation and, in flotation, of electron and ion transfer between the solid and the liquid or gaseous phases.

In mineral beneficiation the phenomena most favorable to separation are best achieved if (a) the system of different phases is as far as possible from equilibrium conditions and (b) the evolution of the surface energy structure towards undesirable stable conditions, which are scarcely beneficial or even unfavorable to the separation, are retarded or avoided. Several techniques are available to induce modification in mineral surface energy levels. These include the action of the modulating agents, heat treatment, X- or radioisotope irradiation, neutron or ion bombardment, doping by solid diffusion under controlled conditions, type of comminution triboelectric charging before flotation [10, 11].

The Fermi level, derived from Fermi-Dirac statistics, may be taken as characterizing, in terms of average behavior, an energy structure that may be very complex. It represents the mean energy of the electrons involved in the interphase exchanges that occur in electric or electrochemical phenomena. The Fermi level is closely related to the thermodynamic or chemical potential. The position of the Fermi level, or the corresponding potential, determines the charge transfer direction across the interface of two solid phases.

Plakala and Shafeey [11], were the first to demonstrate the possibility of using electronic defects for increasing the separation efficiency in flotation and tribo-electrostatic separation, and have since been followed by a number of other authors. In triboelectric charging between two bodies in contact, that body having the upper Fermi level, i.e., the lower work function, gives electrons to the other; thus, after separation of the bodies, it will be positively charged leaving the other negatively charged [9].

In flotation, adsorption phenomena are influenced by the position of the Fermi level. Adsorption of anions on the surface of a given mineral may be hindered or its probability diminished by enhancement of the Fermi level by external actions; the opposite occurs if cations are involved.

The position of the Fermi level, although it determines the direction to which the system evolves, has scant influence in determining the entirety of the resulting effect. If the concentration or the mobility of the charge carriers is too low, the exchanges will be limited and the contribution from the crystal bulk will be small.

The third one is the effect of ionizing radiation. The effect of the radiation such as X-rays, γ -rays and α -rays can be considerable. All the types of radiation are found to give rise to a displacement of the Fermi level with respect to the natural untreated mineral.

The fourth one is effect of ionic bombardment and triboelectric charging in flotation. Although ionic bombardment enhances flotation yield for all the species, triboelectric charging exhibits a rather more selective action.

J

SECTION II

THEORY

We can consider a perfect crystal as one with a completely ordered structure having its atoms at rest (except for zero-point oscillation at the absolute zero temperature) and with the electrons distributed in the lowest-energy states. But, actually, there are several types of deviations or imperfections which may occur. The typical one is increased amplitude of random movement of the atoms about their equilibrium rest points as the temperature is increased.

Imperfections also occur in the electronic energy levels; electrons may be excited into higher energy levels, leaving vacant positions in the normally filled electronic energy-level bands, called electron holes. There are a number of atomic defects [3], including substitution of a wrong atom or a foreign atom for a normal one, and line imperfections called dislocations (Figure 1). It has recently been established that the properties of a real crystal are a function not only of its composition and lattice type, but also of the deviations from the regular structure that appear in the process of its generation.

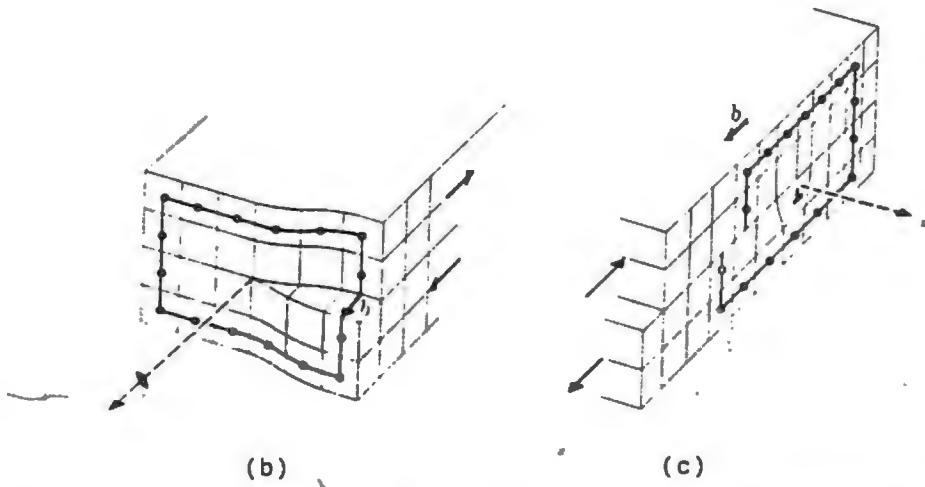
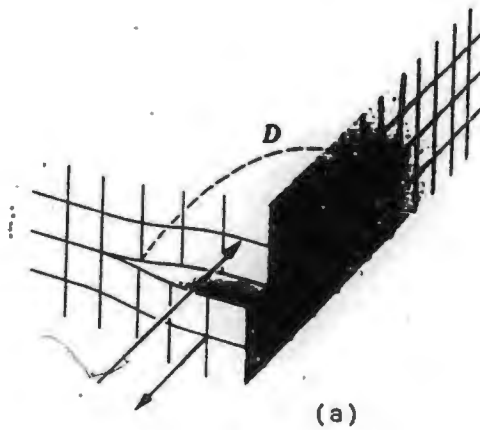


Figure 1. (a) Shear dislocation. The dislocation loop, D , is a line of disregistry. All other unit cells match their neighbors. (b) Screw. (c) Edge. The displacement is parallel to the screw dislocation but perpendicular to the edge dislocation.

Following Van Buren[3,19], the crystallographic defects can be divided into four groups according to their dimensions (Figure 2).

In an ideal crystal, in addition to all atoms being on the right sites with all sites filled, the electrons should be in the lowest-energy configuration. Because of the Pauli exclusion principle, the electron energy levels are limited to a number of energy bands up to some maximum cutoff energy at 0°K which is known as the Fermi energy $E_f(0)$. At higher temperatures thermal excitation gives an equilibrium distribution in some higher energy states so that there is a distribution about the Fermi level $E_f(T)$ which is the energy for which the probability of finding an electron is equal to one-half. Only a small fraction of the total electron energy states are affected by this thermal energy depending on the electron energy band scheme[20].

The different temperature effects[4] observed for metals, semiconductors, and insulators are related to the electronic energy band levels (Figure 3). In metals, these bands overlap so that there is no barrier to excite electrons to higher states. In semiconductors and insulators a completely filled energy band is separated from a completely empty conduction band of higher electron energy states by a band gap of forbidden energy levels.

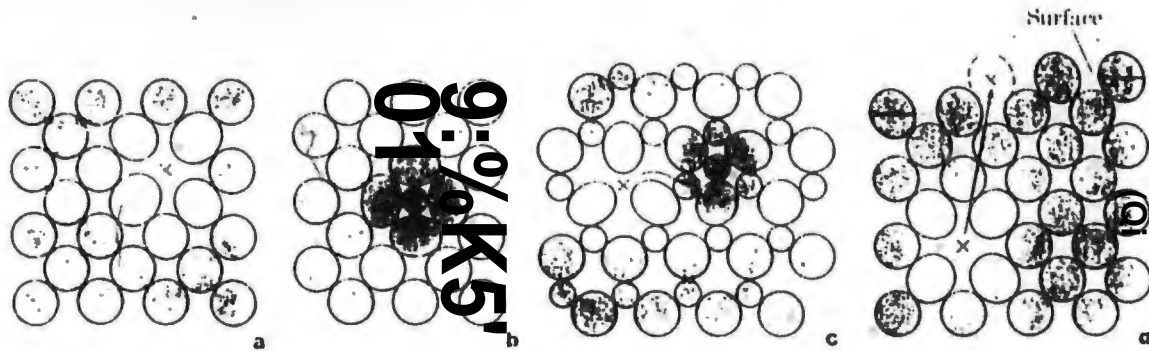


Figure 2. Point defects. (a) Vacancy. (b) Interstitial. (c) Displacement to the interstitial site (Frenkel defect). (d) Displacement to surface. An imperfection distorts the crystal lattice.

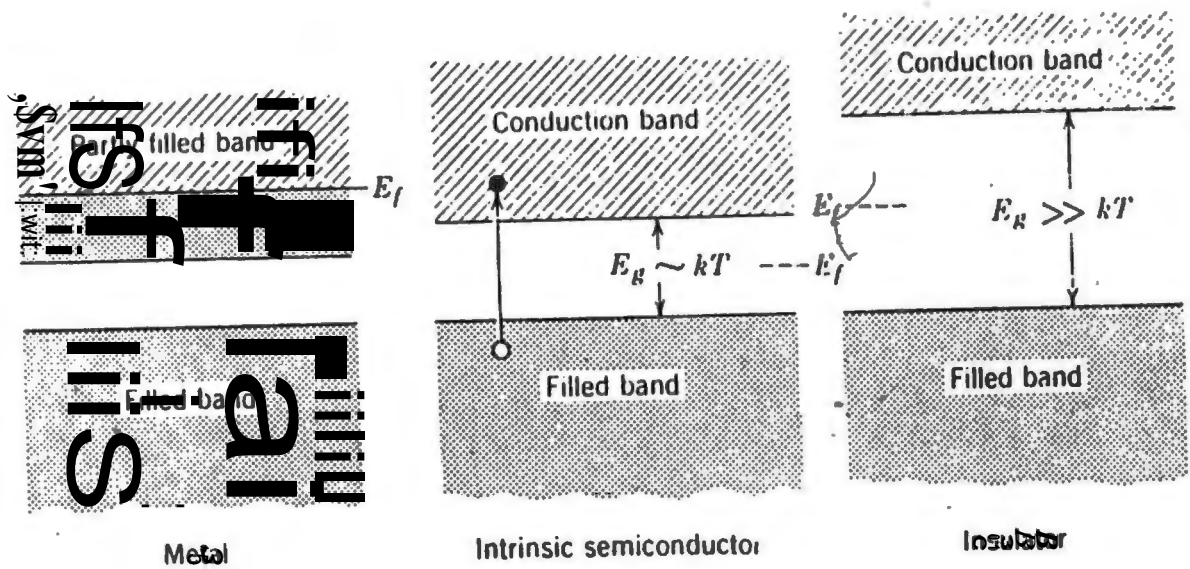


Figure 3. Electron energy band levels for metals with partly filled conduction band, intrinsic semiconductors with a narrow band gap, and insulators with a high value for E_g .

In intrinsic semiconductors the energy difference between the filled and empty bands is not large compared with the thermal energy, so that a few electrons are thermally excited into the conduction band, leaving empty electron positions (electron holes) in the normally filled band. In perfect insulators the gap between bands is so large that thermal excitation is insufficient to change the electron energy states, and at all temperatures the conduction band is completely devoid of electrons and the next lower band of energy is completely full, with no vacant states.

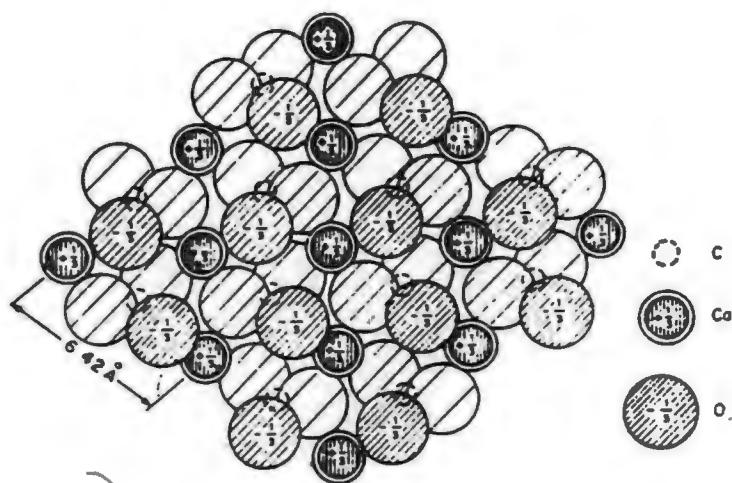
In an intrinsic semiconductor, each electron whose energy is increased so that it goes into the conduction band leaves behind an electron hole, so that the number of holes equals the number of electrons, $p = n$. The nomenclature usually employed is to indicate the positive electron-hole concentration by p , and the negative excess electron concentration by n .

In this case the Fermi level E_f is half way between the upper limit of the filled band and the lower level of the conduction band.

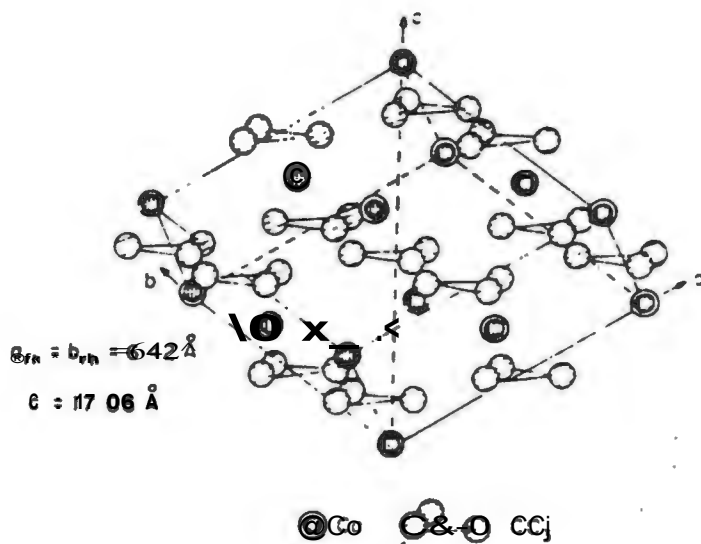
The Fermi level can be taken as characterizing, in terms of average behavior, an energy structure that is very complex. It represents the energy of electrons involved in the interphase exchanges that occur in electrical or electrochemical phenomena. The concentration of the intrinsic electronic defects can be calculated. In this calculation the thermal randomization of electrons is related to the probability of a valence electron in the full band having enough energy to jump across the energy gap E_g into the conduction band.

Crystal structures of carbonates, sulfates, tungstates, and phosphates are much more complex than those of simple structures such as fluorites. In these former cases, cations are ionically bonded to anionic radicals which are composed of several non-metallic species strongly bonded to each other by mixed ionic and covalent forces. The most common carbonate mineral, calcite, possesses a rhombohedral structure[5] with the Ca^{++} ions located at the corners and faces of the unit cell and the CO_3^{--} ions located at the center of both edges and the cell itself (Figure 4).

Each cation is coordinated in the structure to six oxygen atoms of six different CO_3^{--} groups. The aragonite form of $CaCO_3$ is characterized by a coordination number of nine for its cation and an orthorhombic crystal structure.



(a)



(b)

Figure 4. (a) Surface structure of calcite (1011),
(b) Crystal structure of calcite.

The position of the Fermi level for semiconducting minerals can be determined in two different ways using two separate series of tests. The first is the measurement of the contact potential difference between the mineral sample and a gold reference electrode using the modified Kelvin method, both the vibrating and rotating condenser being used as the measuring devices. This method, which has been briefly described in earlier papers[8,9], allowed the measurement of the work function for different materials[17]. Measurement of the work function makes it possible to confirm that the sign of the triboelectric charge depends on the relative position of the Fermi level of the two substances in contact and that a correlation exists between collector adsorption and mineral work function[17].

The second method consists of the determination of the Fermi level, E_f , once E_g is known, by measurement of the thermoelectric power (Seebeck coefficient) ($mV/^\circ K$) by using the following equations[21]:

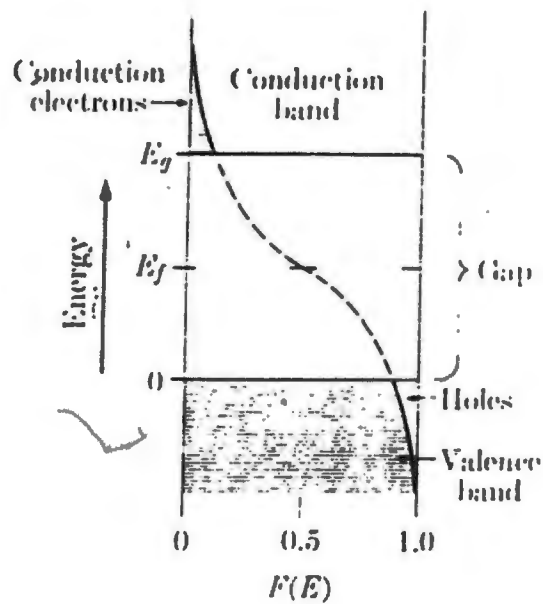
$$\text{thermoelectric power; } Q = -k/q \quad (A = \mu) \quad (1)$$

$$\mu = E_g - E_f / kT \quad (2)$$

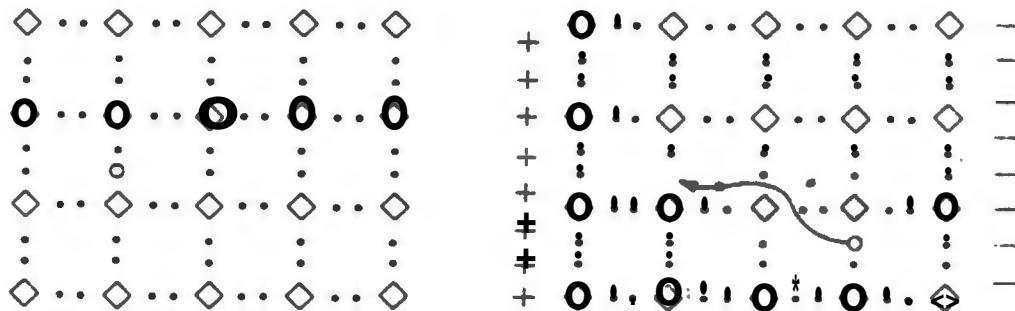
In the Equation(1) the positive sign holds for p-type semiconductors and the negative sign for n-type semiconductors. The constant A is assumed equal to 2 because of scattering processes arising from the thermal vibrations of the lattice atoms. Q is the thermoelectric power. q is the charge of the electron. This method, which gives the position of the Fermi level with respect to the upper edge of the valence band, is adopted in the present work to find out the correlation between electric separation or flotation results and displacement of the Fermi level as a result of external actions (Figure 5).

Of the two methods available for determination of the position of the Fermi level, the first, which allows indirect measurement of the work function ϕ , is more suitable in studying the charge transfer process between two different bodies, whereas the second, which gives E_f , is preferable when the effect of different actions on the same mineral is to be investigated.

The second method is known to be more versatile, as it can be applied also to powdered mineral samples. This is a distinct advantage in the study of flotation phenomena. The width of forbidden band E_g is determined by measuring the electrical conductivity σ as a function of temperature.



(a)



(b)

Figure 5. (a) Fermi distribution (intrinsic semiconductor). Since an intrinsic semiconductor has as many holes as conduction electrons. (b) Hole conduction. The hole, 0, moves toward the negative electrodes as if it were a positive charge.

In the intrinsic field the relationship between σ and T can be approximately written as

$$\sigma = \sigma_0 \exp(-E_g / kT) \quad (3)$$

where E_g is obtained. σ_0 is a conductivity constant determined by experiment.

Thermoelectric power is calculated as a function of temperature in the range 250 °K to 600 °K. If the thermoelectric power is attributed entirely to electronic effects, one can calculate its temperature and pressure dependences in a manner analogous to that used to calculate the temperature and pressure dependence of the conductivity[23]

$$n_e = K \exp(-E_g/2kT) PO_2^{-1/n} \quad (4)$$

where n_e is the number of electrons per cm^3 , K is equilibrium constant (calcite, 4.7×10^{-9}), E_g is the forbidden energy gap, k is Boltzmann's constant, T is the absolute temperature, PO_2 is the partial pressure of oxygen, and n is a constant.

If the thermoelectric power is given by the relationship [24]

$$\text{thermoelectric power ; } Q = -k/q (2 - \ln (n_e/n_o)) \quad (5)$$

where q is the charge of electron, and n_o is the effective density of states at the band edge

$$n_o = 2(2 m^* kT)^{3/2} / h^3 \quad (6)$$

where m^* is the effective electron mass, then at constant temperature

$$Q = -k/q (\text{Constant} + 1/n \ln PO_2) \quad (7)$$

If the pressure is held constant in Equation (4), then the relation for Q is given by

$$Q = -k/q (\text{Constant}' + \ln n_o + E_g/2kT) \quad (8)$$

In the present work the mass of the electron is used for m^* and the pressure term is ignored. Values of $1/2E_g$ are obtained from the conductivity measurements.

SECTION III

EXPERIMENTAL PROCEDURE

SAMPLE PREPARATION

Mineral samples used were synthetic and natural calcium carbonates obtained from an industrial company plus Iceland spar purchased from Wards Natural Science Establishment, Inc. The particle shapes varied greatly and included angular, blocky and nearly spherical particles[22]. Methods of sample preparation included precipitation from solution and grinding. Particle size of the material varied from about 0.1 to 40 μ m. X-ray analyses indicated that all the materials except for Mississippi Lime were calcite. This material was primarily aragonite with some calcite present[22]. Table 1. lists some of the characteristics of the materials studied.

The powdered samples were mixed with distilled water and pressed in a press, Siaplimet II, Buehler Co. with high pressure(80,000 psi) to make cylindrical samples for good contact between probes and samples. The samples were kept in the oven(Fisher Model 496) at the temperature, 70 °C for 24 hrs to evaporate the water left in the samples after pressing.

Table 1. Characteristics of Calcium Carbonates Studied

Material	Particle Shape	Preparation	Surface Area (m ² /g)	Isoelectric Point
Aldacer	blocky	precipitation	1.7	more than 7
Wicron	block-angular	grinding (naturally occurring mineral)	9.2	10.8
Aldasphere	spherical	precipitation	3.4	9.5
Aldaglo	blocky	precipitation	6.5	9.5
Miss. Lime	elongated-angular	precipitation	10.6	8.2
Utrefine	spherical-blocky	precipitation	20.1	8.3
Iceland spar	block-angular	grinding (naturally occurring mineral)	_____	_____

SAMPLE HOLDER

A diagram of the sample holder used is shown in Figure 6. For better conductance very thin silver foil (.005" VWR Scientific Inc.) was used as a silver plate on each side. The connecting wires from the electrode to the measuring unit were also silver(99.99%), but of a small diameter(0.25mm). They were completely insulated with a silicon tube. The holder was tightened properly to reduce contact problem between sample and plates. The conductivity measurements were made with a high frequency (> 103 Hz) Gen Rad 1658 RLC bridge to avoid polarization of the sample. Conductivity was measured in an inert atmosphere(argon gas).

For the determination of the sample resistance several measurements were made and an average taken. The temperature at which the measurements were made was determined from the thermocouple(Omega Co. K type) connected to a thermocouple thermometer(Omega Co. Model 2168A) (Figure 7). The slope of the resulting curve was determined by the method of least squares. The temperature of the furnace(Lindberg Model 58111) would drift as much as ten degrees centigrade during a twelve-hour period.

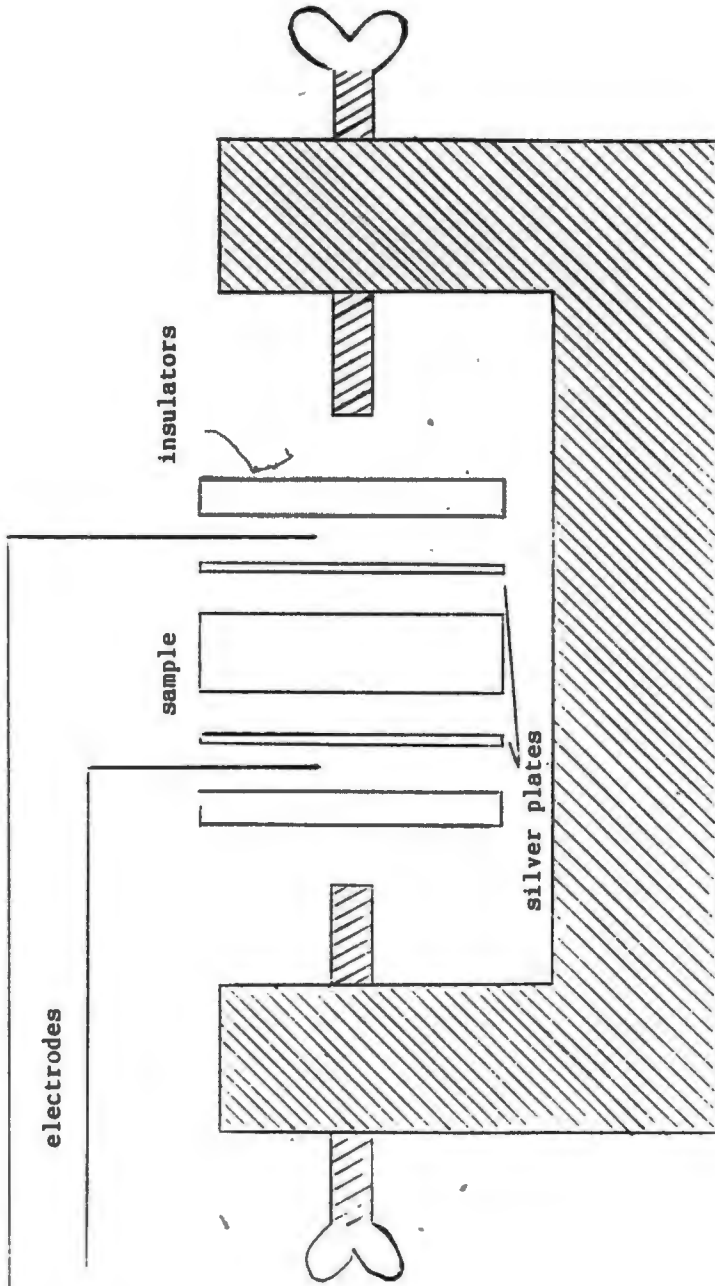


Fig. 6 SAMPLE AND SAMPLE HOLDER

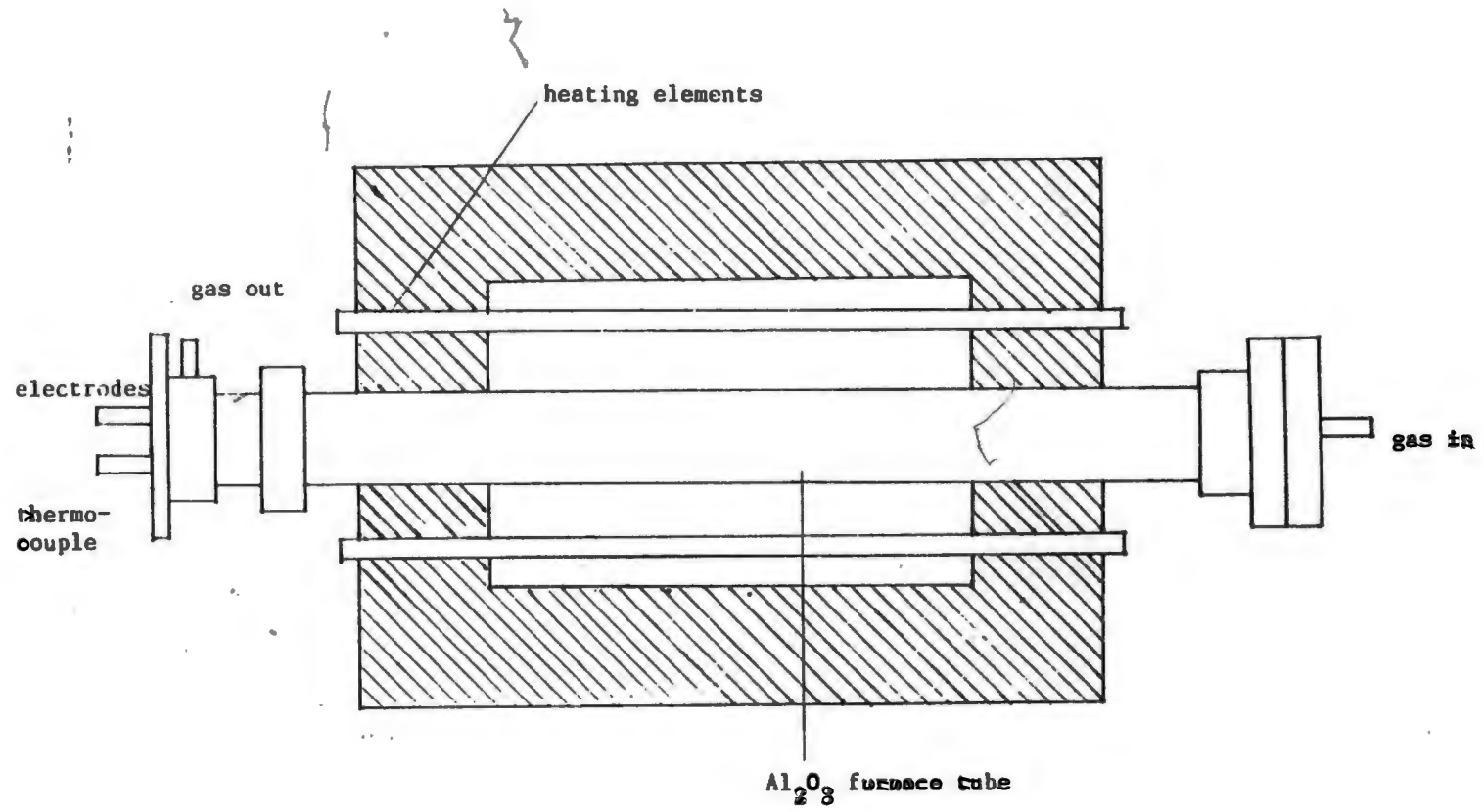


Fig. 7 SIDE VIEW OF THE FURNACE USED

It was found necessary therefore, to take two or three readings about a temperature and then determine the resistance at the temperature desired from the meter.

Considering the relations developed in this section the measured electrical conductivity σ is plotted against $1/T$ for different calcites in Figures 8-14. The forbidden energy gap, E_g , can be determined by measuring the slope of the rectilinear section at the higher temperatures, where the calcite is intrinsic[18]. Figures 16-22 show the variation of the charge carrier concentration in relation to temperatures for various calcites in the intrinsic zone, $p/n = 1$. In the two curves overlap, the Fermi level is situated halfway in the forbidden band.

SECTION IV
RESULTS AND DISCUSSION

Deviations in the crystal lattice of a mineral from the ideal structure can be estimated from data obtained on its electrophysical parameters such as Fermi level or concentration ratio of the charge carriers, p/n , since these parameters do reflect such deviations. The concentration and mobility of the charging carriers of either type is important from this point, and the concentration ratio p/n determines the gradient of the Fermi level as a function of temperature through the relationship.

$$E_f = 1/2 E_g - 1/2 kT \ln p/n \quad (9)$$

where E_f is the Fermi level referred to the upper edge of the valence band, E_g is the width of the forbidden energy gap, k is Boltzmann's constant and T is absolute temperature. The equation reveals the important role played by the forbidden band, the width of which represents the maximum shift of position of the Fermi level attainable through external actions capable of modifying the carrier concentration ratio p/n . A mineral characterized by a very narrow forbidden band is generally little sensitive to various external actions.

The previously observed correlation with flotation response is attributed to the dependence of adsorption of the flotation reagents on minerals on such properties as Fermi level, which is indicative of the mean energy of the surface electrons[17]. To determine the Fermi levels for several calcites the thermoelectric value of each sample was used with equations noted in the previous sections.

The value of the forbidden energy gap, E_g , is necessary for determining the Fermi energy, E_f . Conductivity measurements were performed versus reciprocal absolute temperatures for various calcites and slopes taken over the intrinsic zone, $p/n=1$. Figure 15 shows conductivity measurement data on calcite from Carta, M. et al.[5]. The initial slope gives the value of E_g . In Figures 8-14 the curves were determined by measuring σ (reciprocal to resistivity) at increasing temperatures starting from room temperature. These figures show somewhat different curve shapes but all show similar trends. The slopes taken at high temperatures (intrinsic zone) were similar to that of Carta, M. et al.[5]. These authors also obtained cooling curves showing a hysteresis phenomenon. This was not possible in the present experimentation because of contact problem between the sample and probes. Measured E_g values ranged from 2.168 eV for Mississippi Lime, to 2.31 eV for Iceland spar.

The values were very close to the 2.28 measured by Carta, M. et al.[2]. It means there is no big change in conductivity values and, therefore, E_g values (Figures 8-14) with type of sample preparation.

The charge carrier concentration ratio p/n in the intrinsic zone can be calculated from Equation (10) once the values of E_g and E_f have been determined. The concentration of electrons and holes can be calculated from the relationship

$$np = (2UT^{3/2}) \exp(-E_g / kT) \quad (10)$$

which is, at a given temperature, an invariant of the material (in the present experimentation, calcite) depending on the forbidden gap width only, n is the concentration of electrons (cm^{-3}) and p is the concentration of holes (cm^{-3}). U is a constant of value $2.42 \times 10^{15} \text{ cm}^{-3} \sigma_K^{-3/2}$.

Figures 16-22 show the variation of the charge carrier concentrations in relation to temperatures. In the intrinsic zone, in which $p/n = 1$, the two curves overlap, and the Fermi level is situated half way in the forbidden band.

They are all similar because of the similar E_g values ranging from 1.17 cm^{-3} for Mississippi Lime, to $4.03 \times 10^{10} \text{ cm}^{-3}$ for Iceland spar using Equation (10).

In the thermoelectric power calculations Equations (6-10) were used and the calculated values ranged from -7 eV to -11 eV. The values were then used for the determination of Fermi energy levels. The calculated Fermi energy levels showed all the materials, regardless of manner of sample preparation, to be "n" type semiconductors. They ranged from 4.9 eV to 7.8 eV as temperature is increased. In some earlier papers [1,2] Plaksin, et al. and Carta, et al. the position of Fermi level (Figure 23) is shown decreasing to $1/2 E_g$ as temperature is increased.

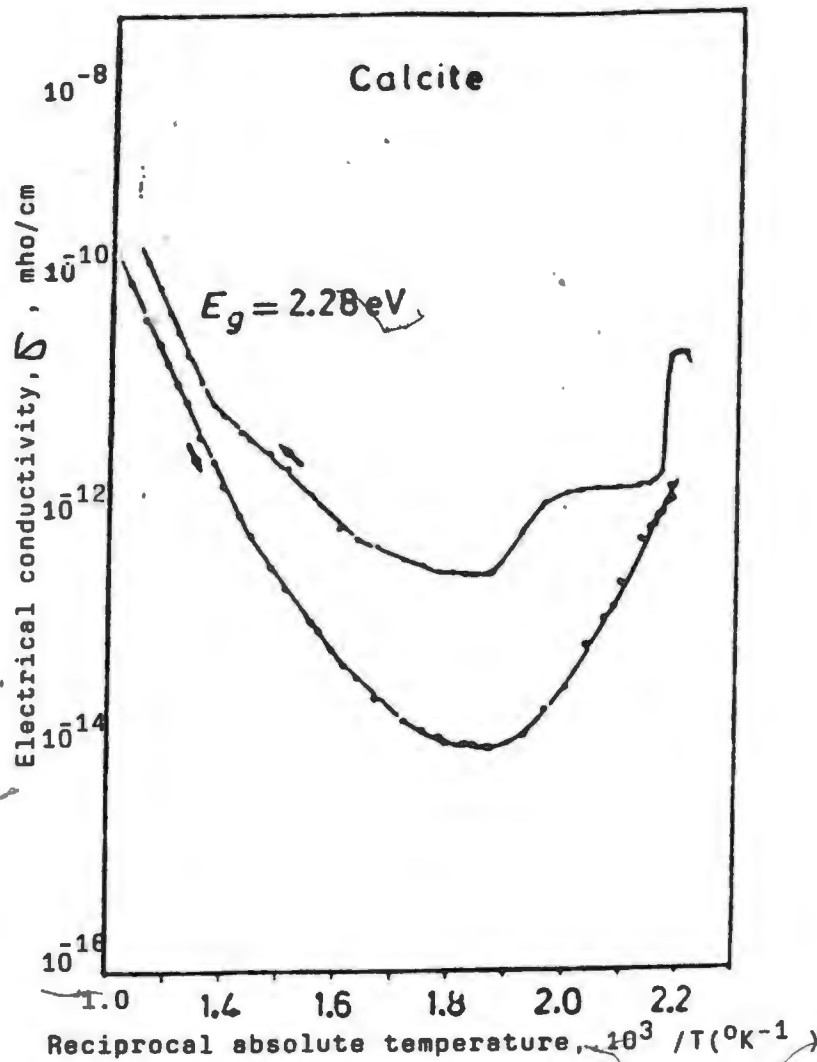


Figure 15. Electrical conductivity versus reciprocal absolute temperature for calcite (size, $-150 + 37 \text{ Mm}$). From Carta, et al. [5].

Figure 8. Electrical conductivity versus reciprocal absolute temperature for Iceland spar (size, 0.1 to 40 Mm).

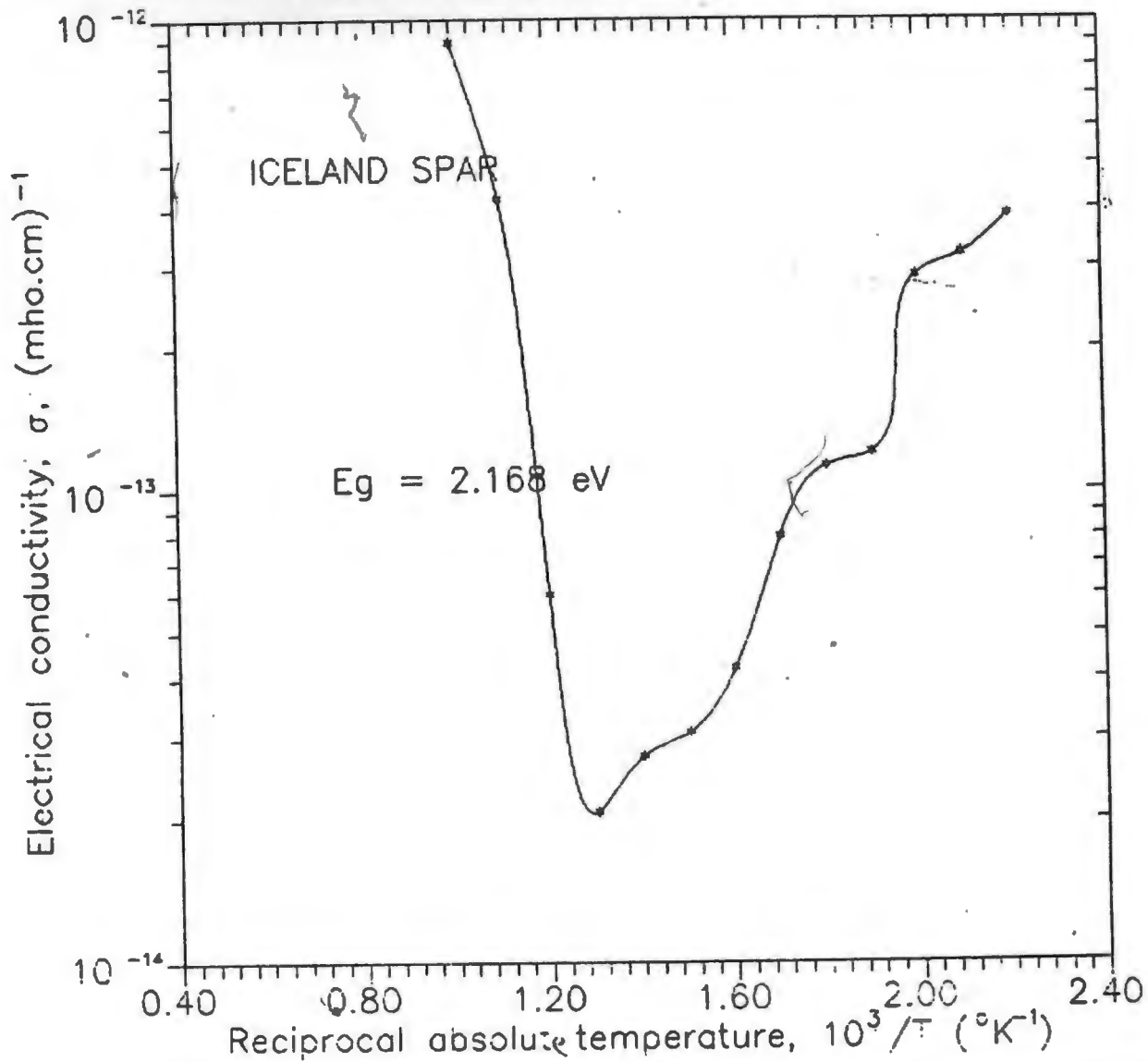


Figure 9. Electrical conductivity versus reciprocal absolute temperature for Albasphère (size, 0.1 to 40 Mm).

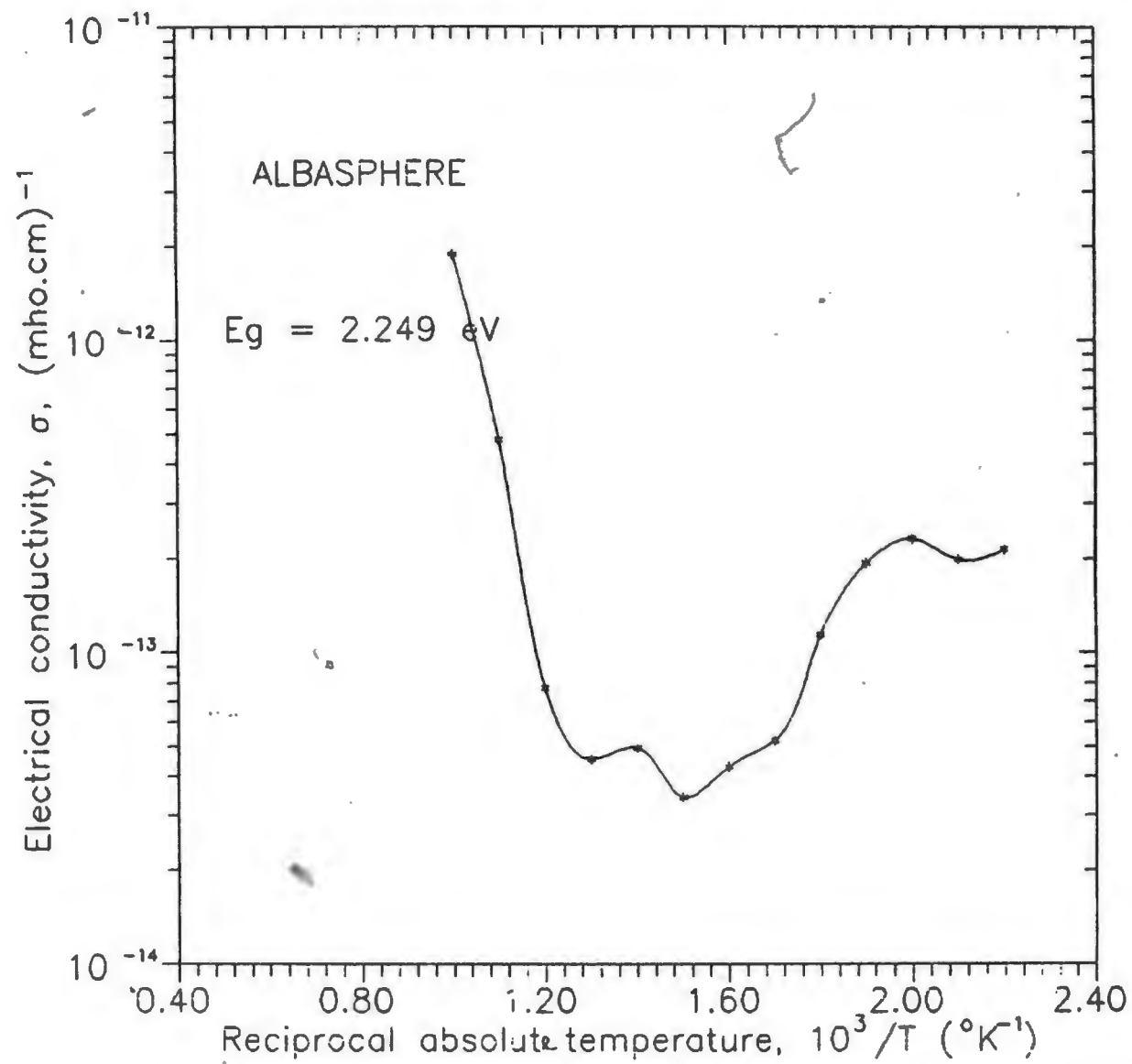


Figure 10. Electrical conductivity versus reciprocal absolute temperature for AlBACAR (size, 0.1 to 40Mm).

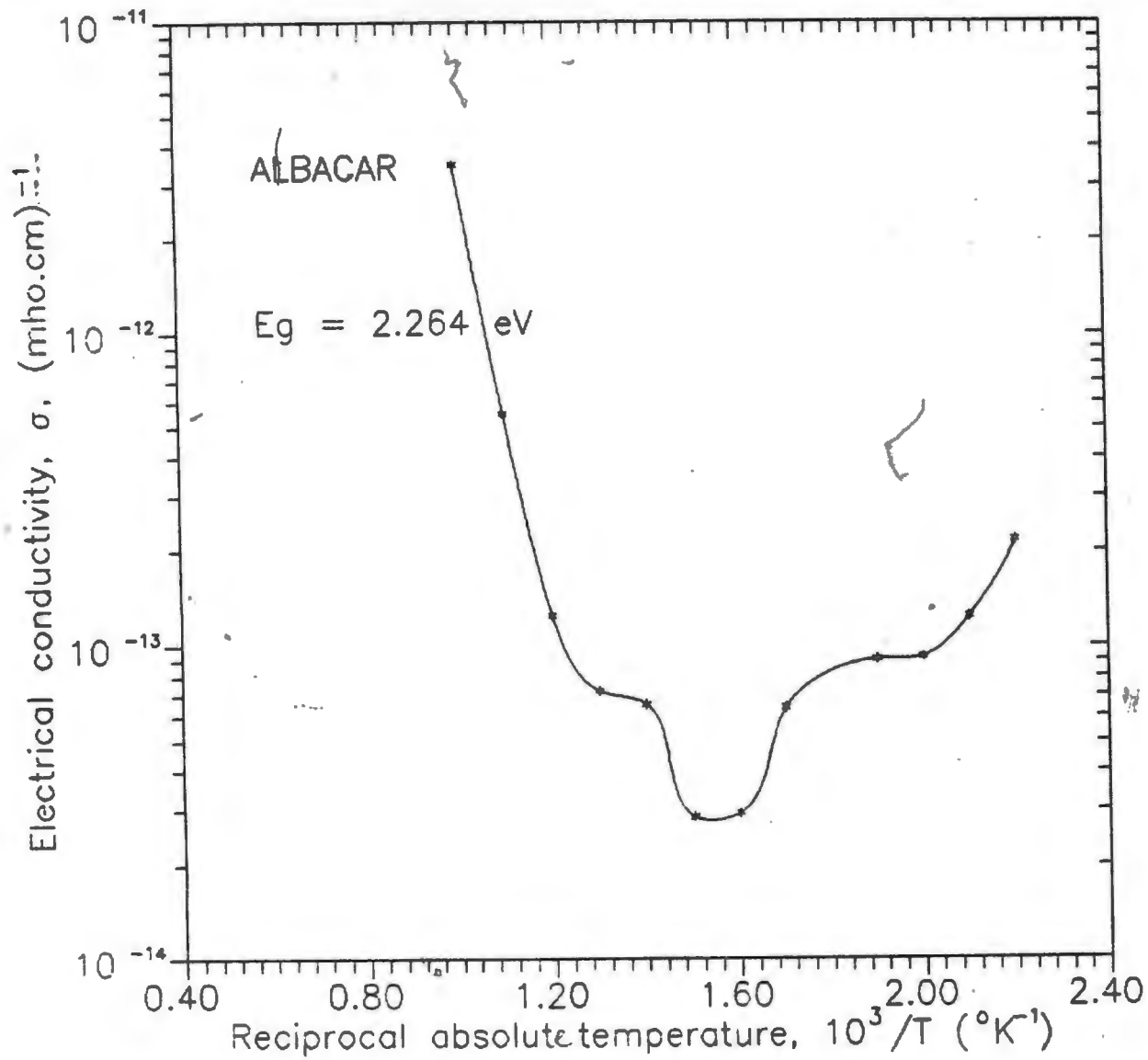


Figure 11. Electrical conductivity versus reciprocal absolute temperature for Ultrafine (size, 0.1 to 40M μ).

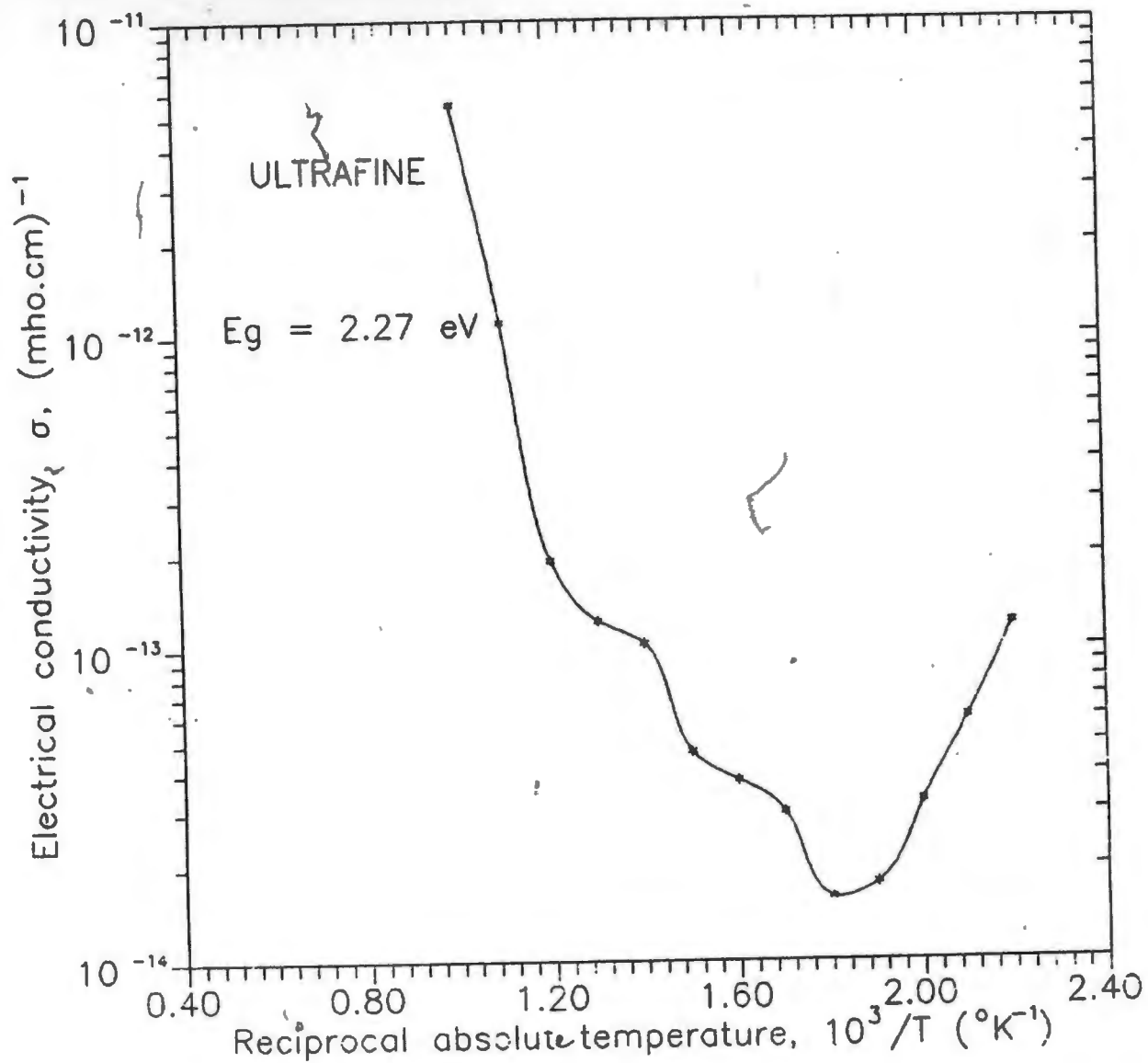


Figure 18. Electrical conductivity versus reciprocal temperature for Albaglos (size, 0.1 to 40 μm).

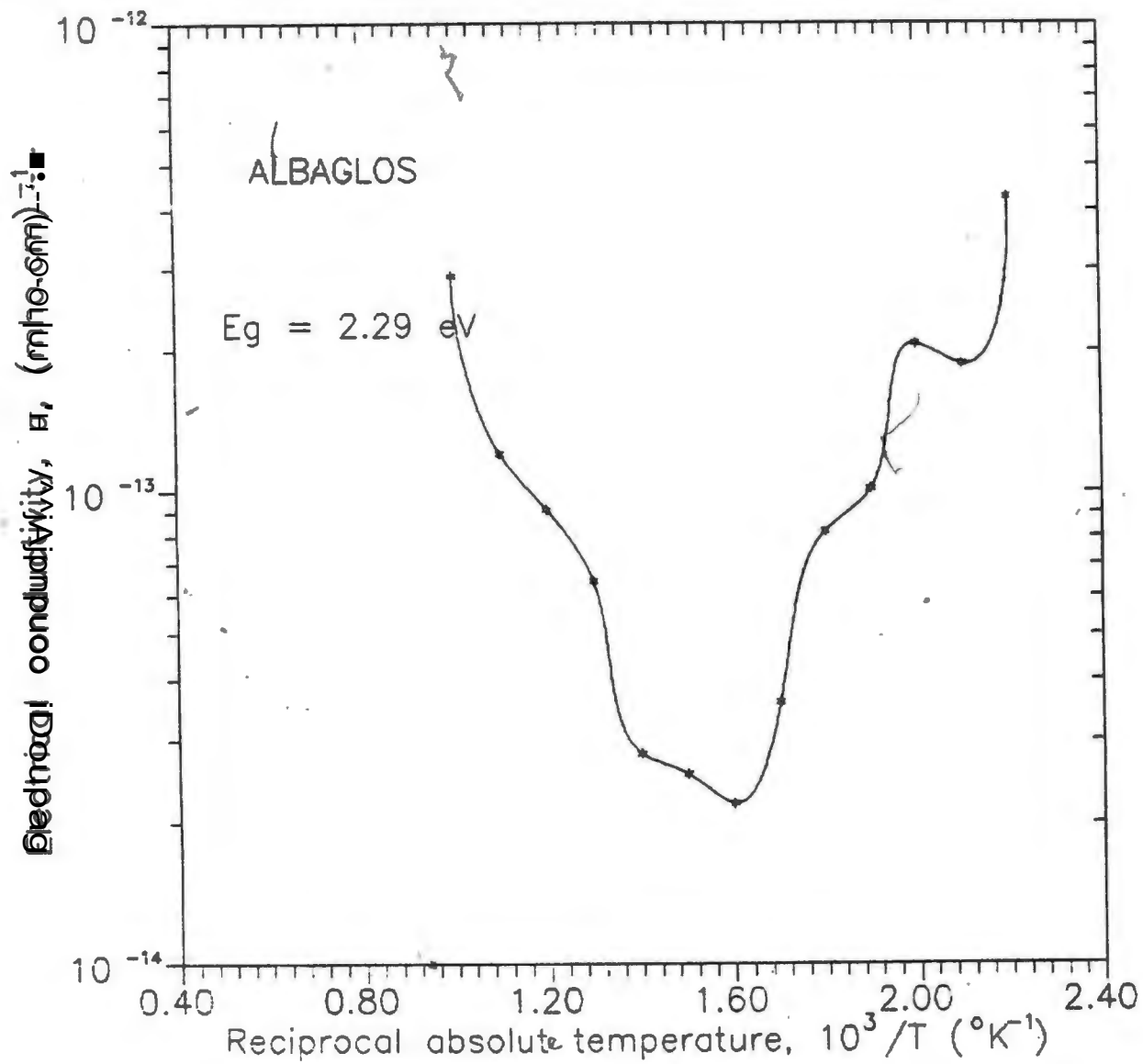


Figure 13. Electrical conductivity versus reciprocal temperature for Vicron (size, 0.1 to 40 Mm).

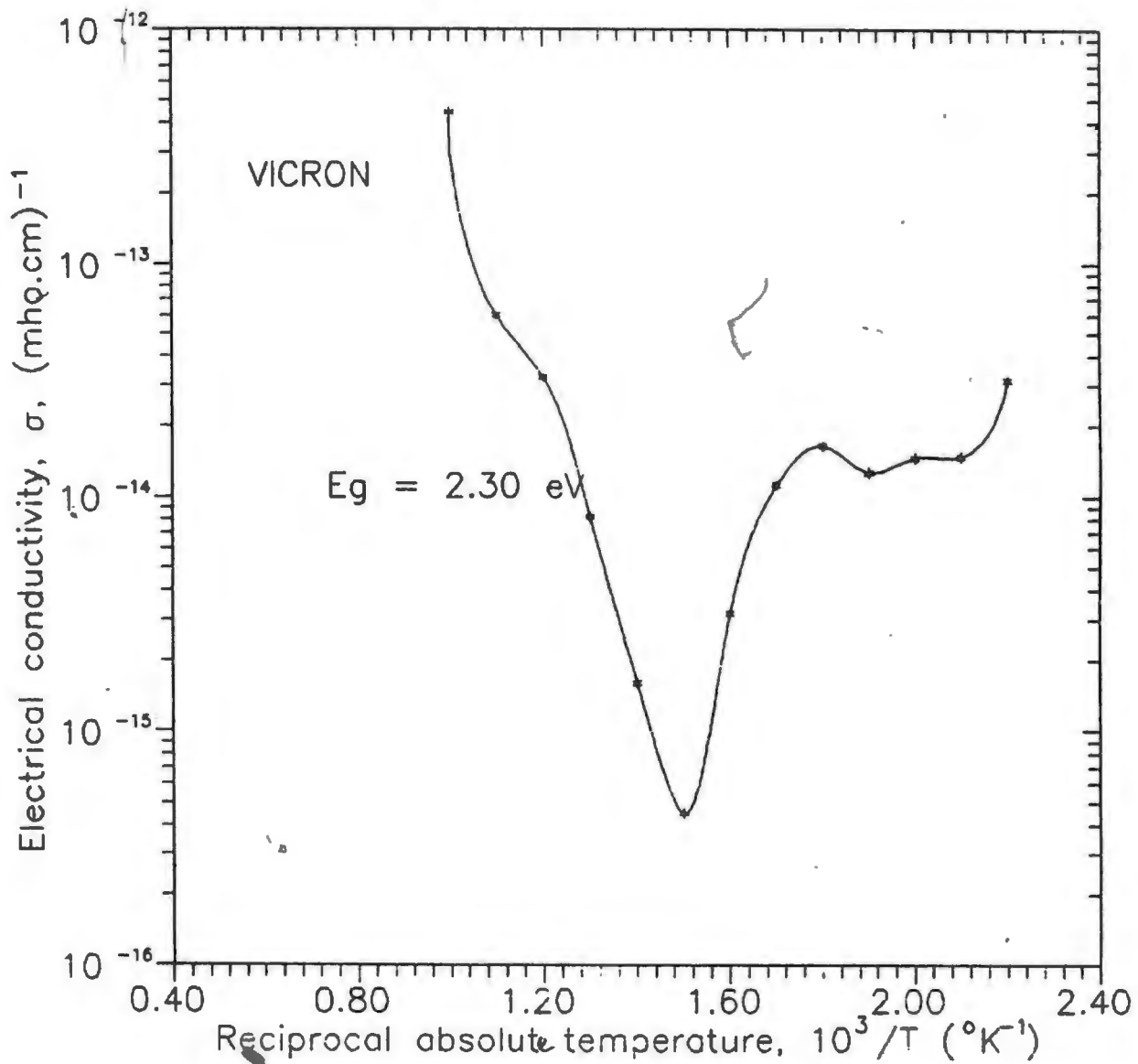
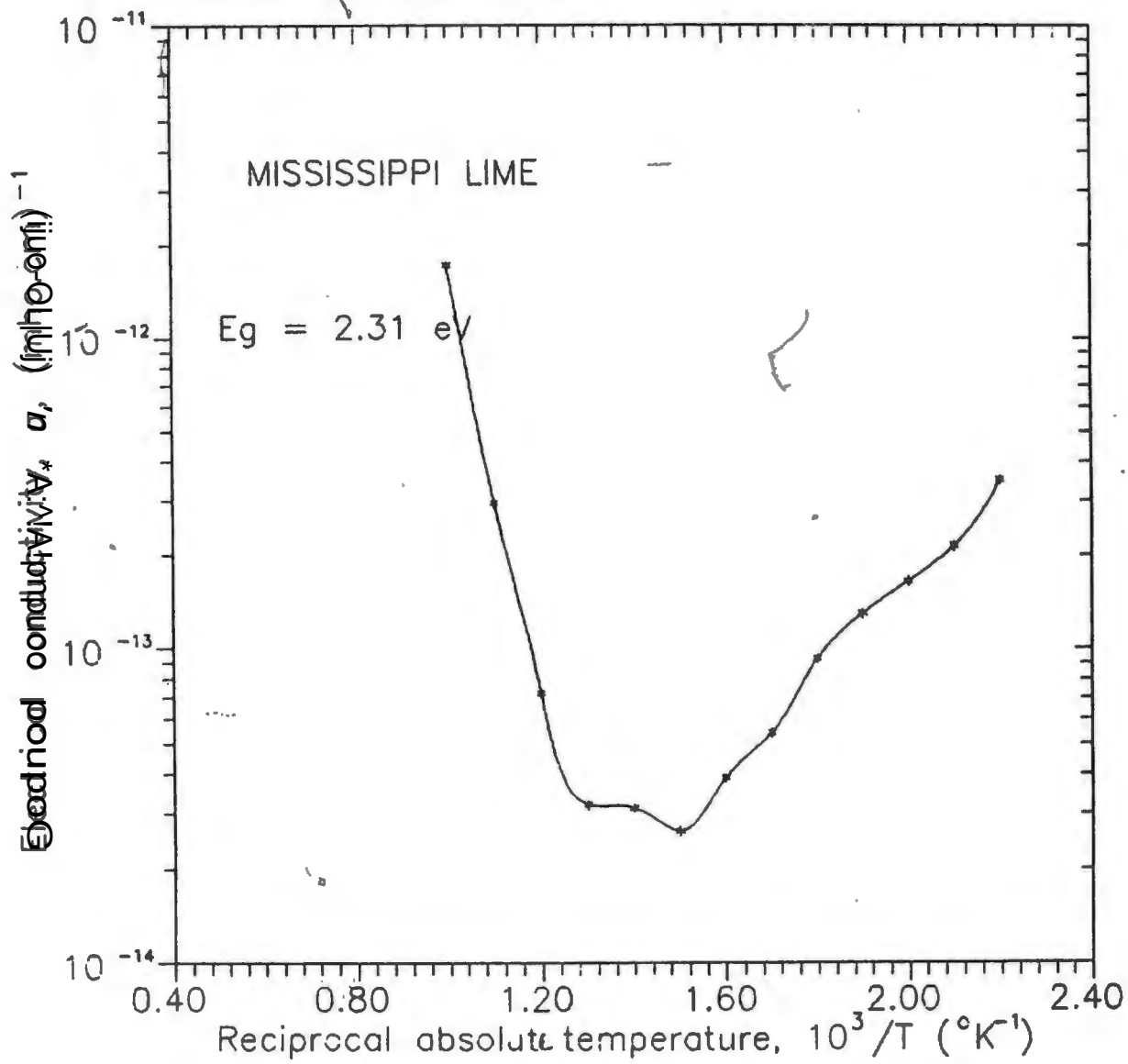


Figure 14. Electrical conductivity versus reciprocal temperature for Mississippi lime (size, 0.1 to 40 Mm).



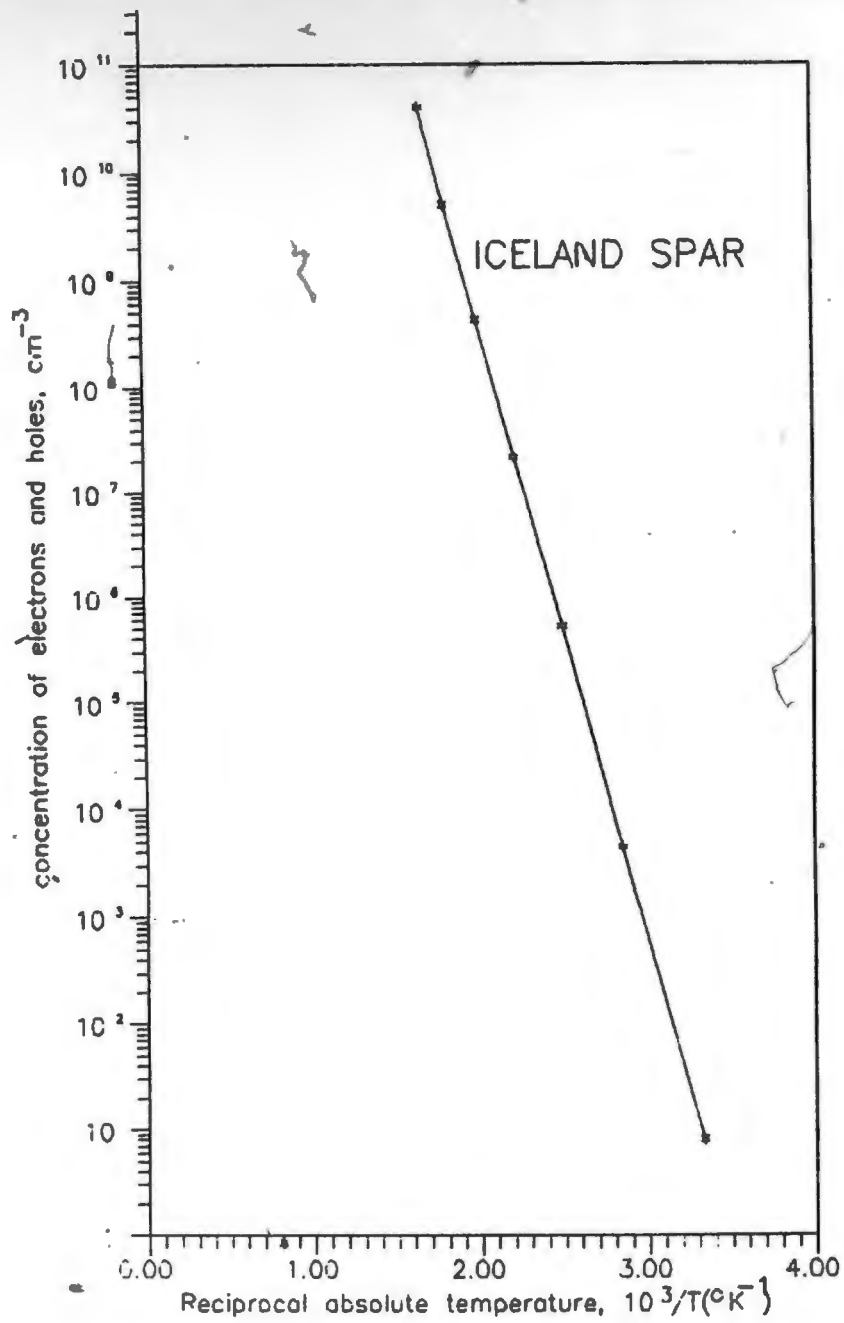


Figure 16. Charge carrier concentration for Iceland spar.

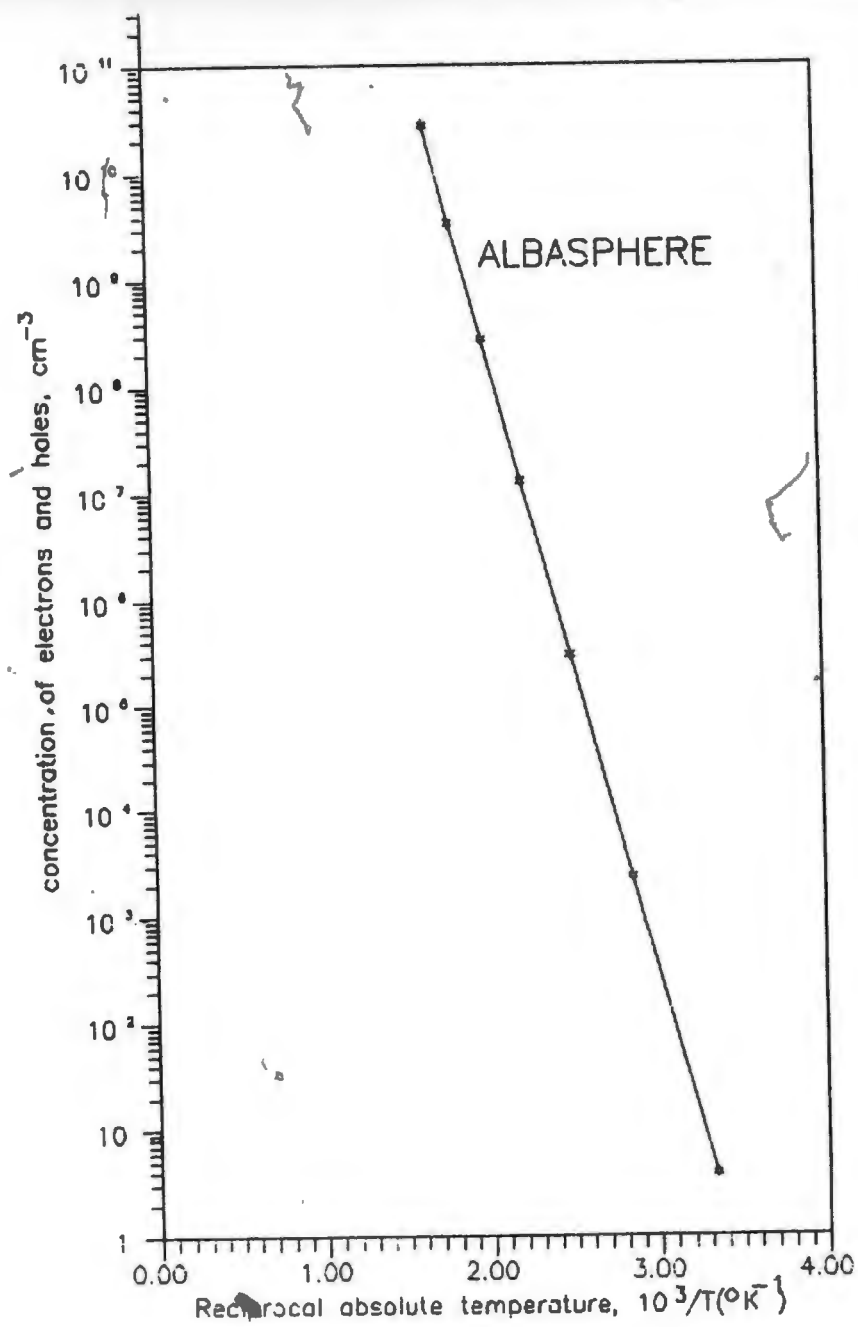


Figure 17. Charge carrier concentration for Albasphere.

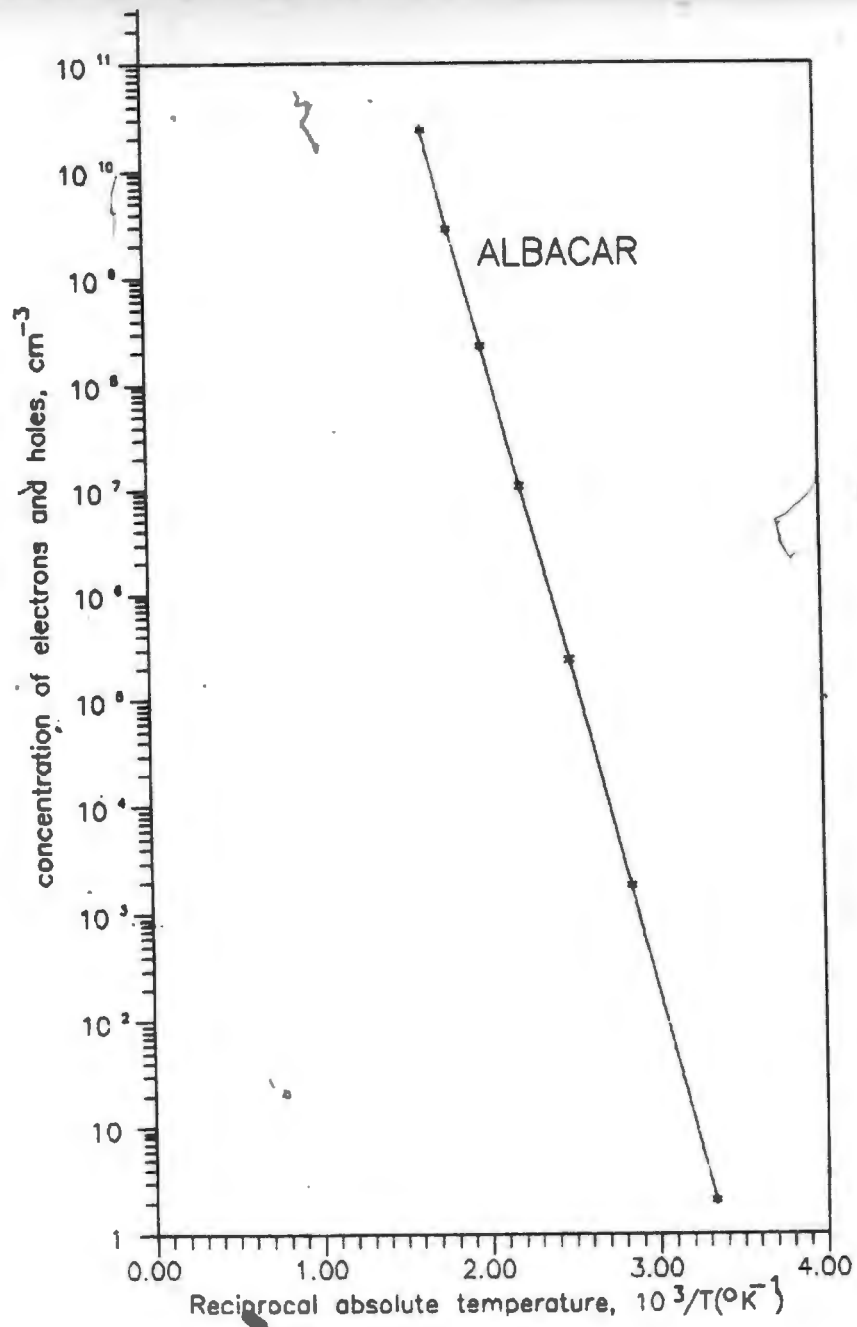


Figure 18. Charge carrier concentration for Albacar.

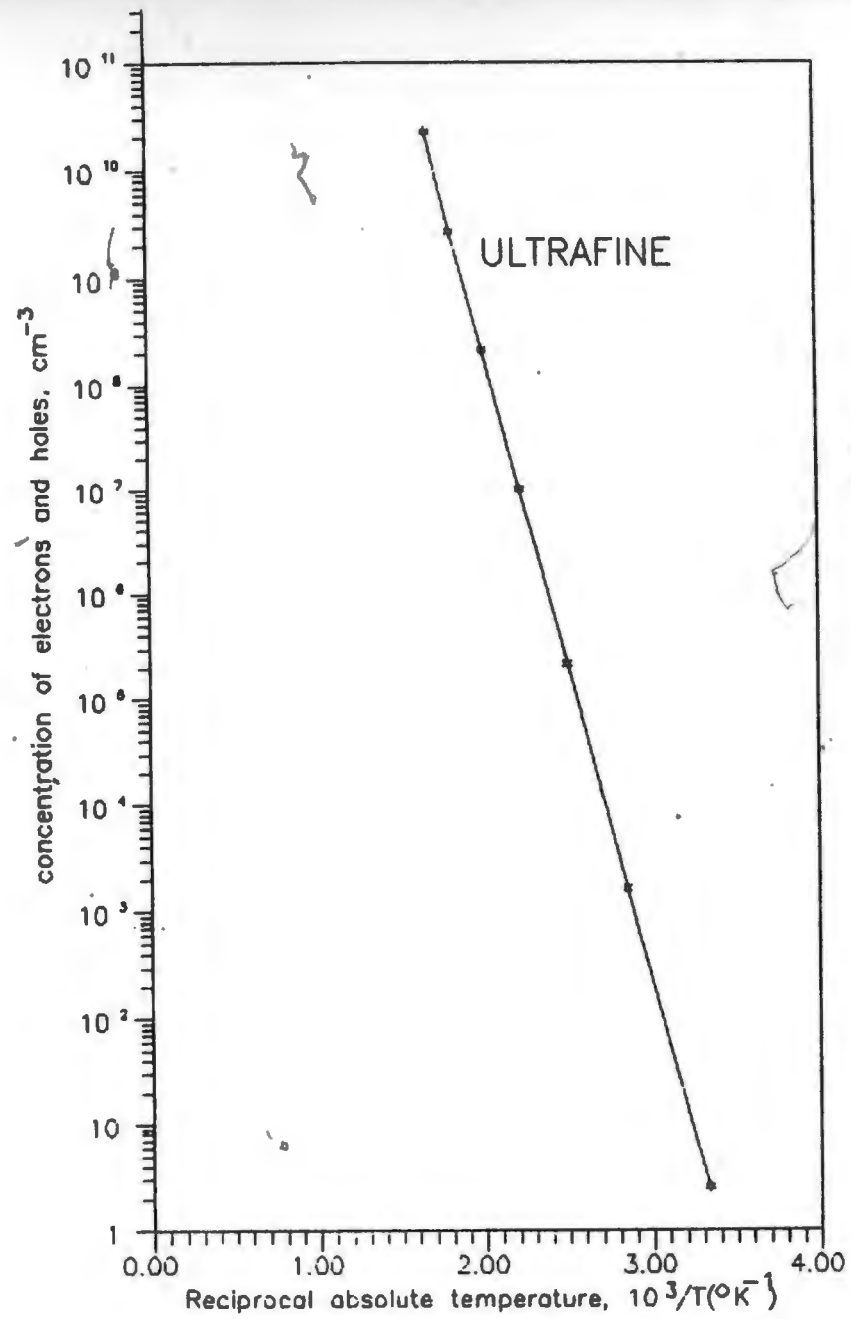


Figure 19. Charge carrier concentration for Ultrafine.

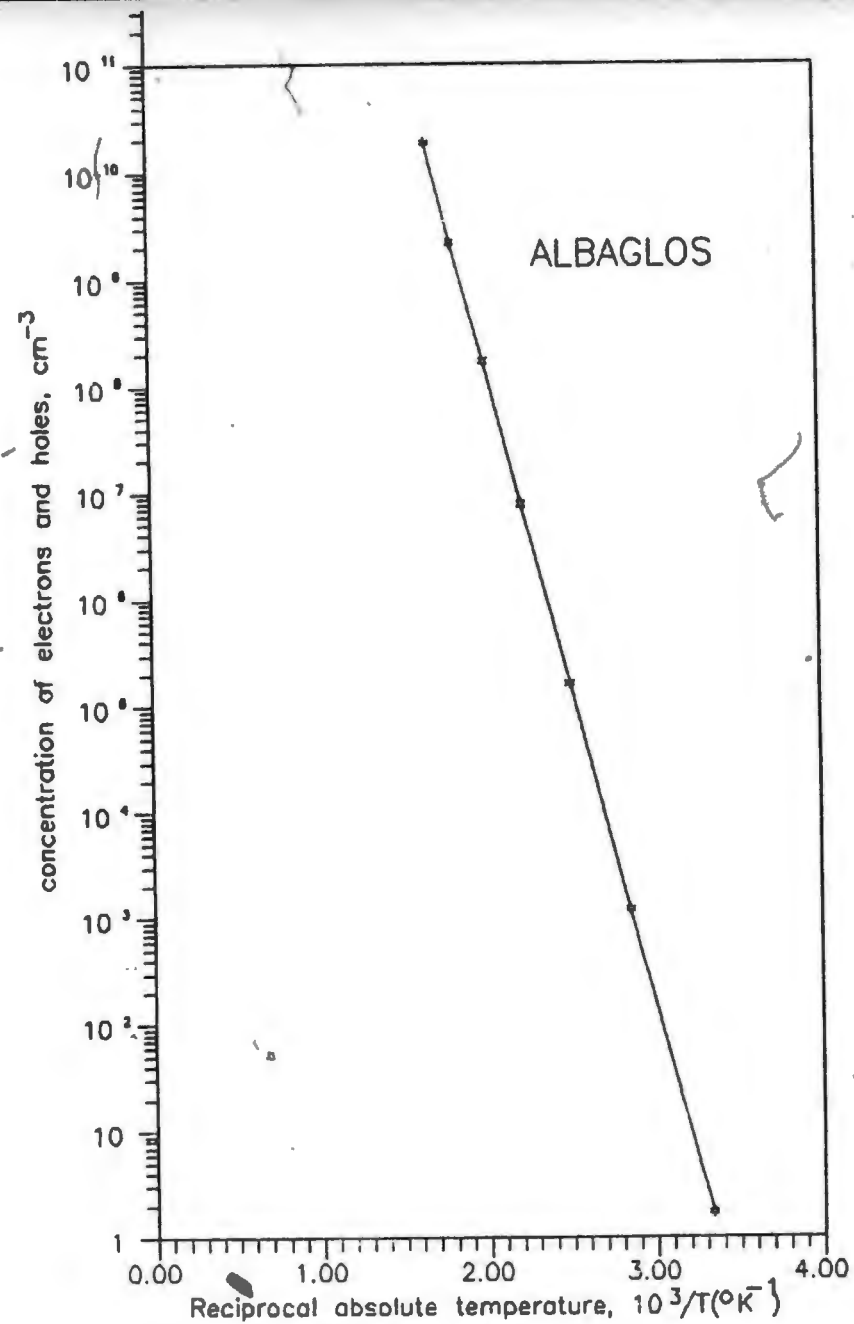


Figure 20. Charge carrier concentration for Albaglos.

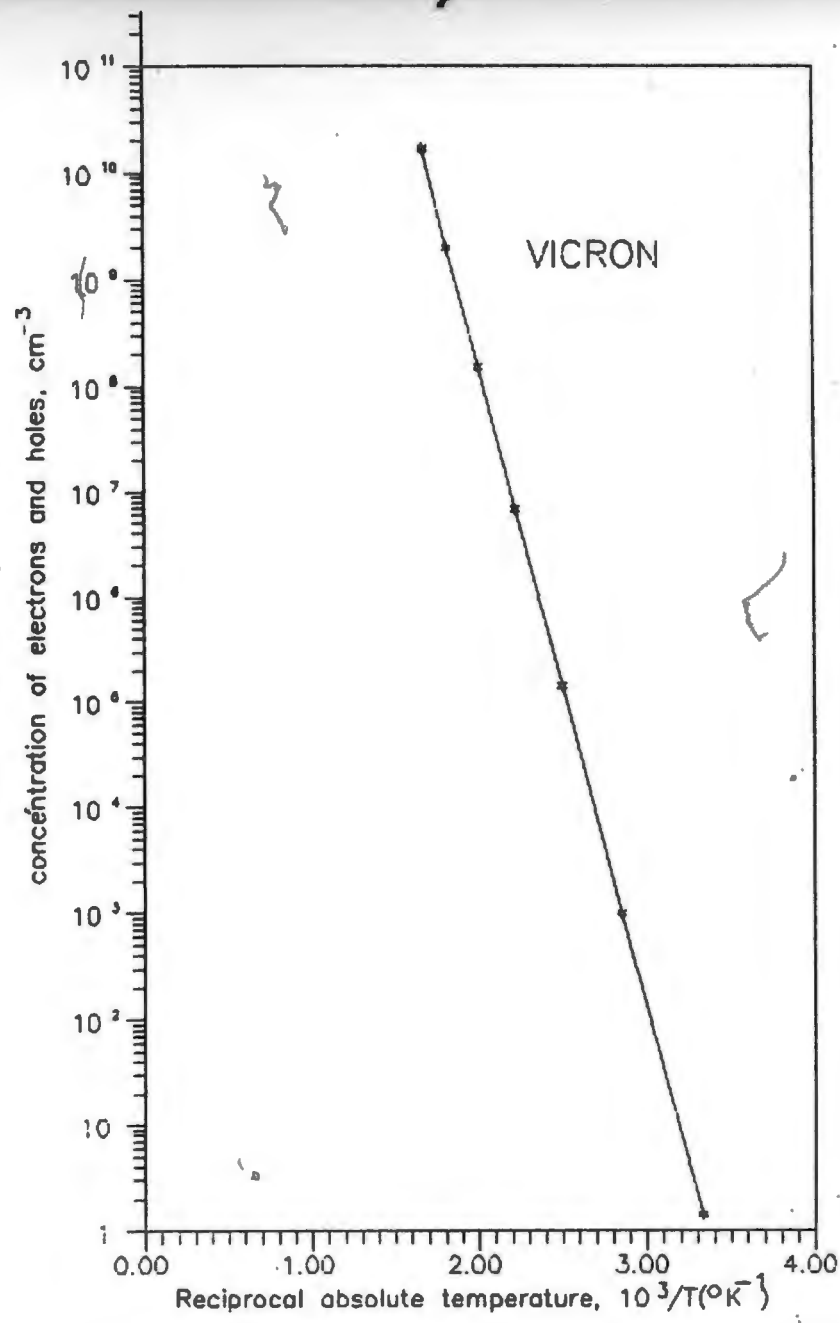


Figure 21. Charge carrier concentration for Vicron.

43

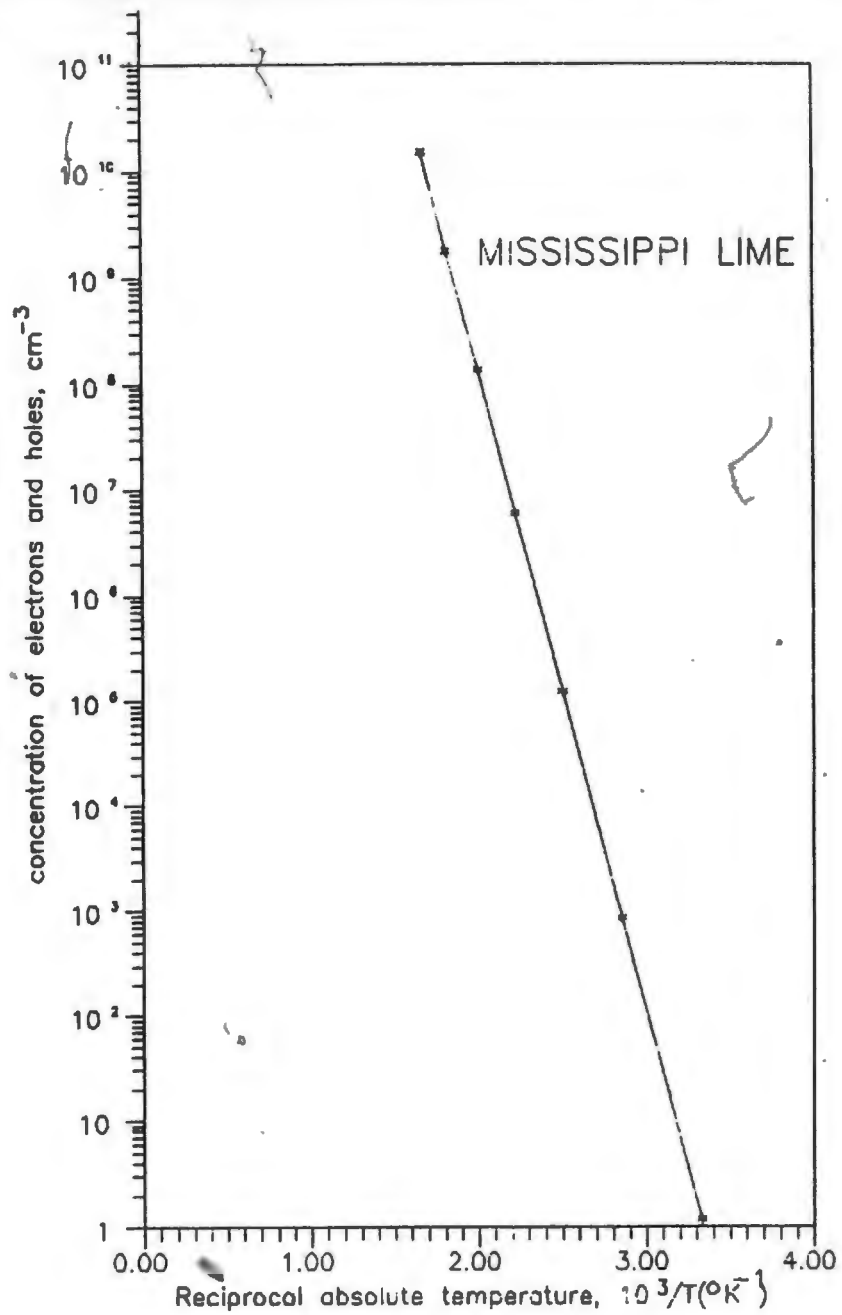


Figure 22. Charge carrier concentration for Mississippi line.

SECTION V
CONCLUSION

The present data (Figures 24-30) show higher Fermi level values for all calcites studied than the data of Carta, et al.[2]. Further, in all present cases Fermi level increased as a function to temperature in the temperature range(200°K - 600°K). For the case of Iceland spar no change in Fermi level was observed when the mineral was prepared by dry grinding instead of wet grinding. Plaksin, et al.[1] and and Carta et al.[2] have also claimed that grinding can cause polymorphic transitions depending upon grinding conditions.

Some factors such as effective masses(m^*) of the various calcites and the pressure term were ignored and mass of electron was used for m^* . Additional x-ray diffraction or other techniques can be used to improve the accuracy of the Fermi level values. However, the corrections should be relatively small.

Thermoelectric power was derived indirectly from electrical conductivity measurements. Several papers[25,26] have reported on different ways for determining the thermoelectric power experimentally and through calculations. These other procedures could give rise to

f:

different results from those of the present experimentation.

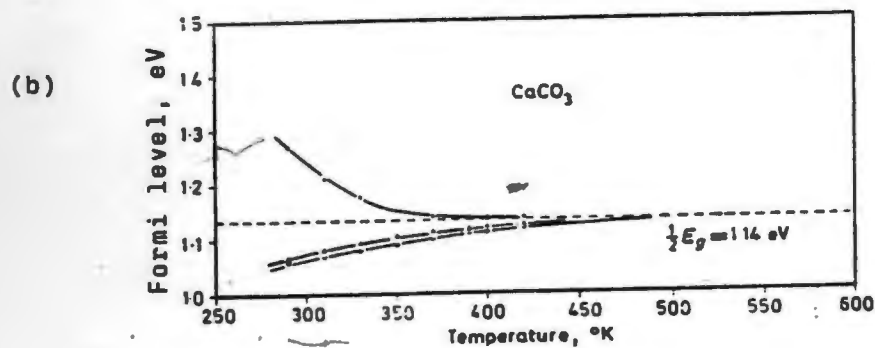
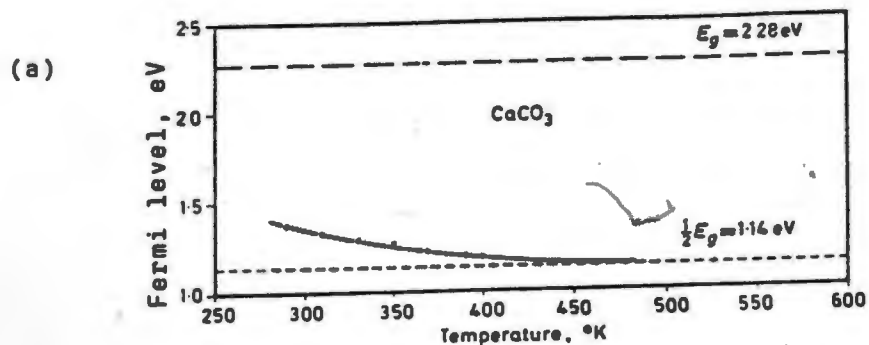


Figure 23. (a) Position of Fermi level as a function of temperature for calcite (size, $\pm 150 + 37 \text{ Mm}$)

(b) Position of Fermi level as a function of temperature at different grinding conditions for calcite (size, -200 Mm ; (1), after dry-grinding (2), after wet-grinding (3), after wet grinding with addition of hydrogen peroxide.

From Plaksin, et al., and Carta, et al. [1,2].

Figure 24. Position of Fermi level as a function of temperature for Iceland spar.

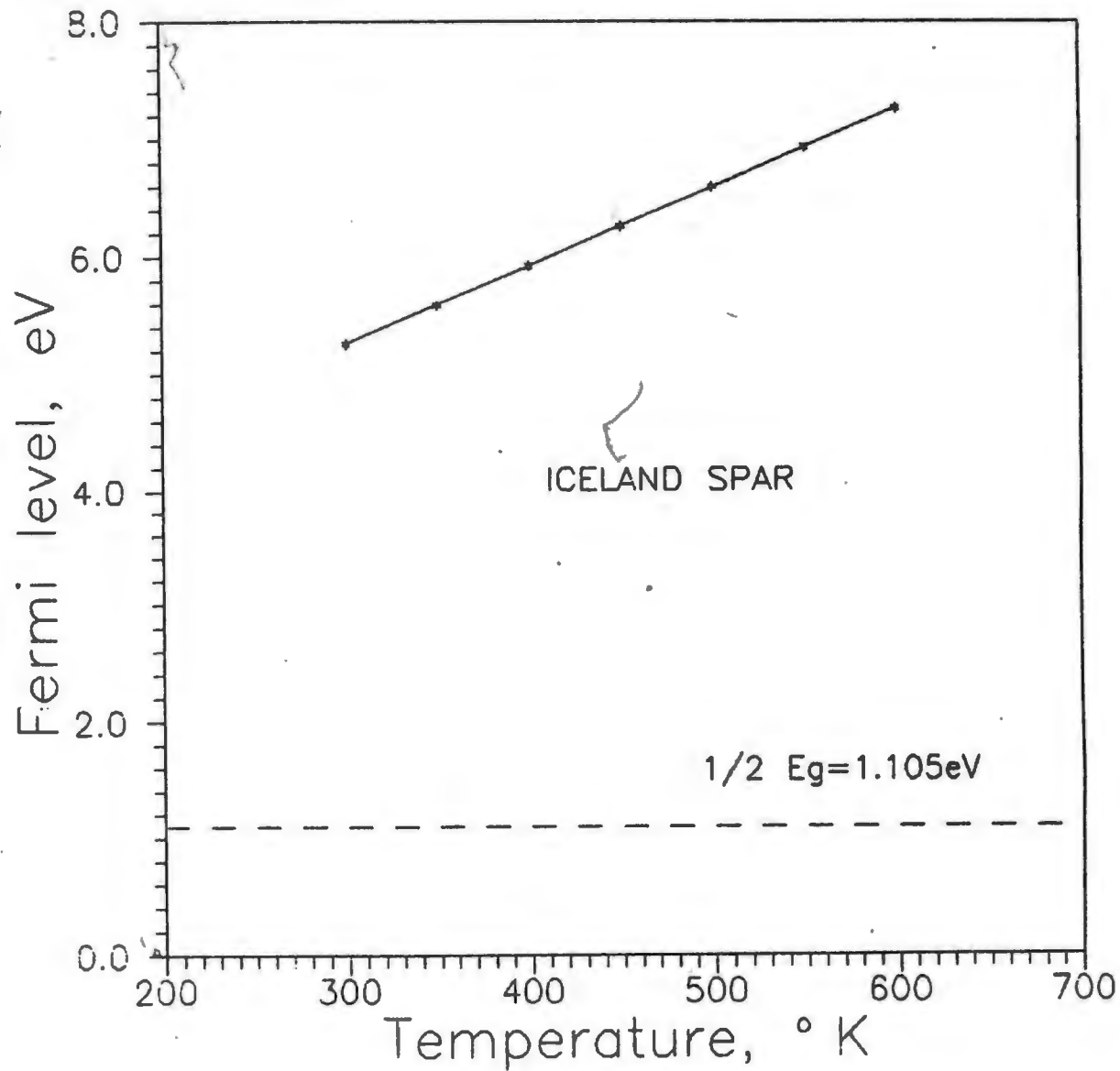


Figure 25. Position of Fermi level as a function of temperature for Albasphere.

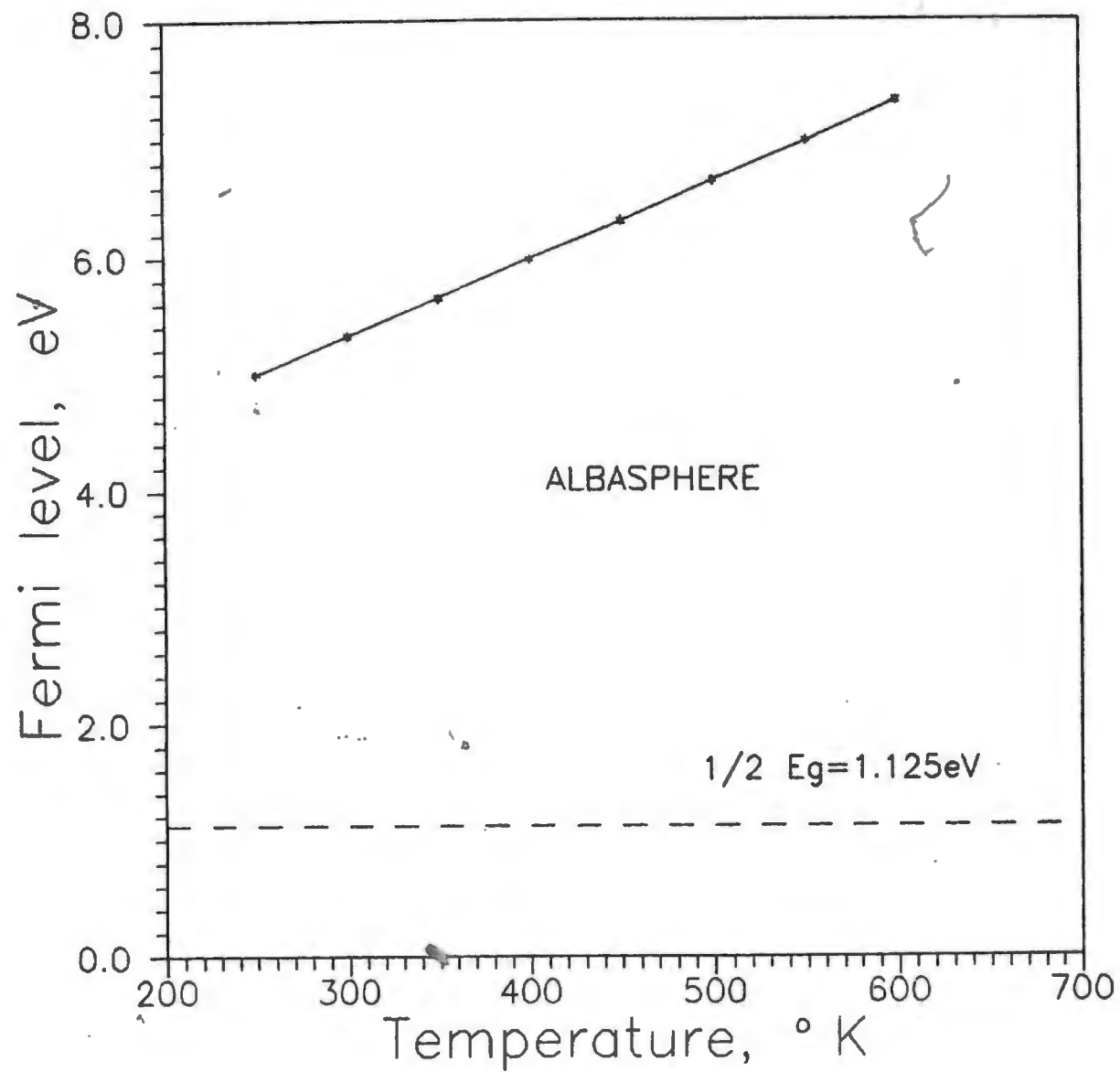


Figure 26. Position of Fermi level as a function of temperature for Albacar.

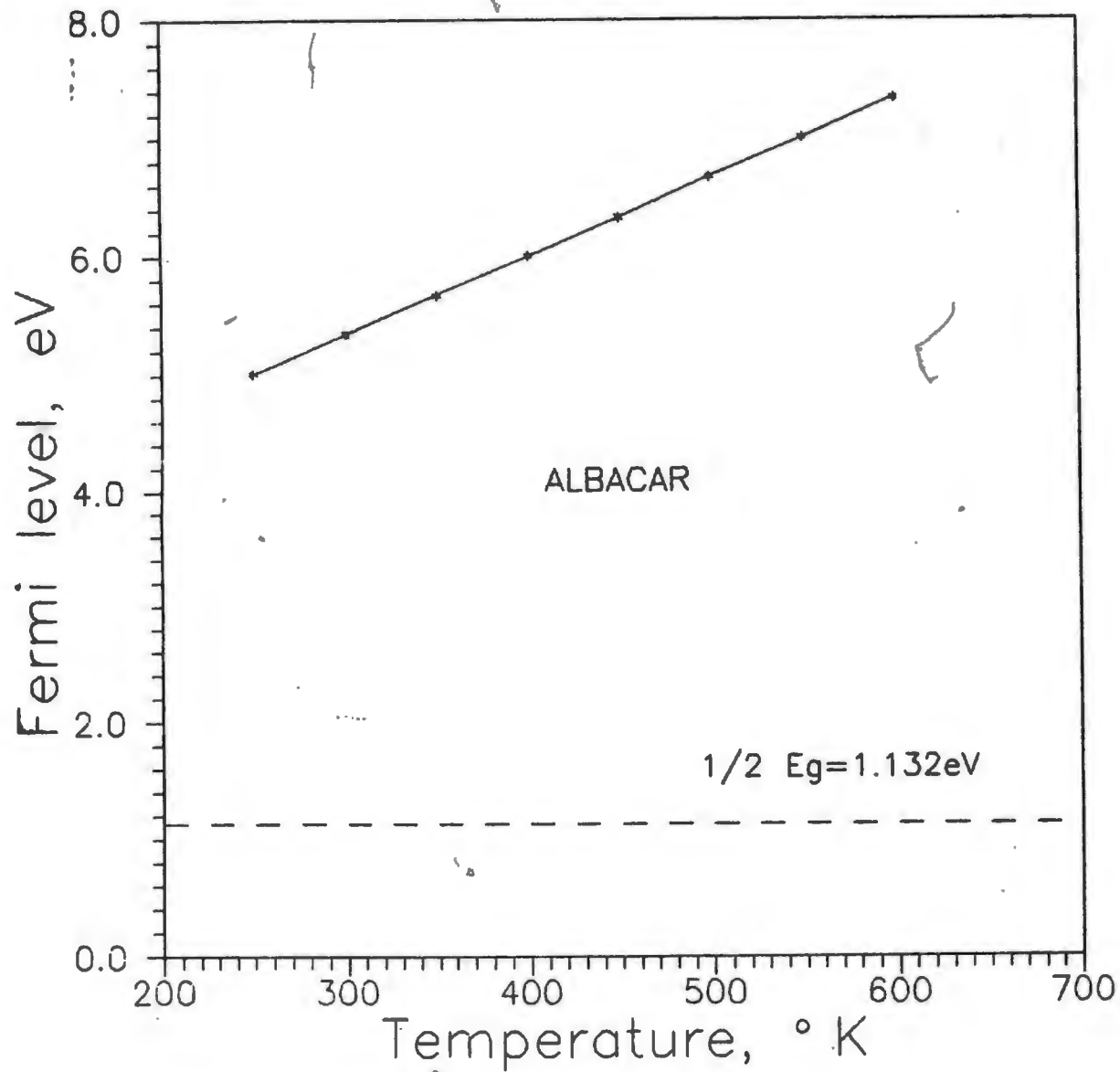


Figure 27. Position of Fermi level as a function of temperature for Ultrafine.

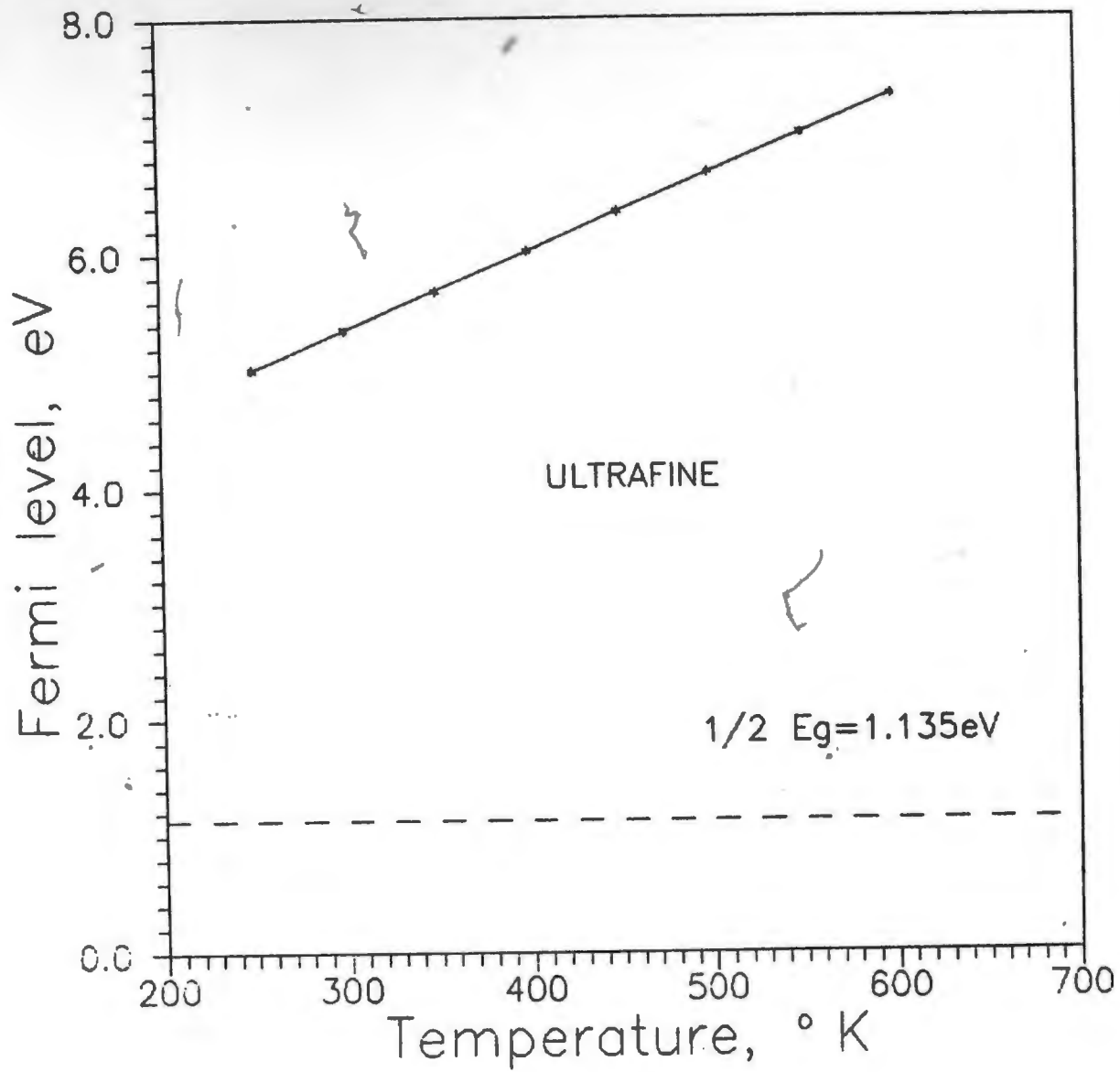


Figure 28. Position of Fermi level as a function of temperature for Albaglos.

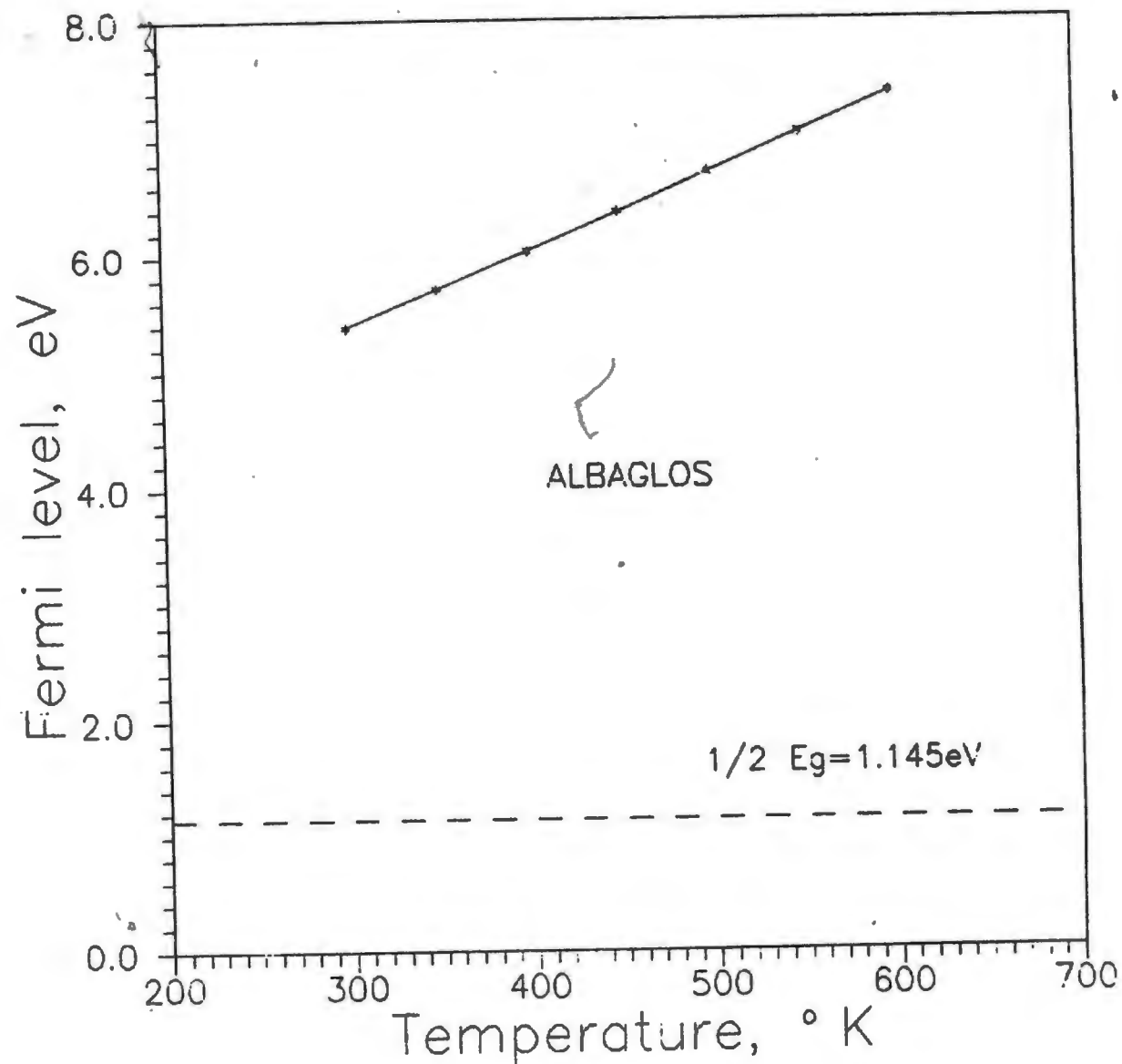


Figure 29. Position of Fermi level as a function of temperature for Vicron.

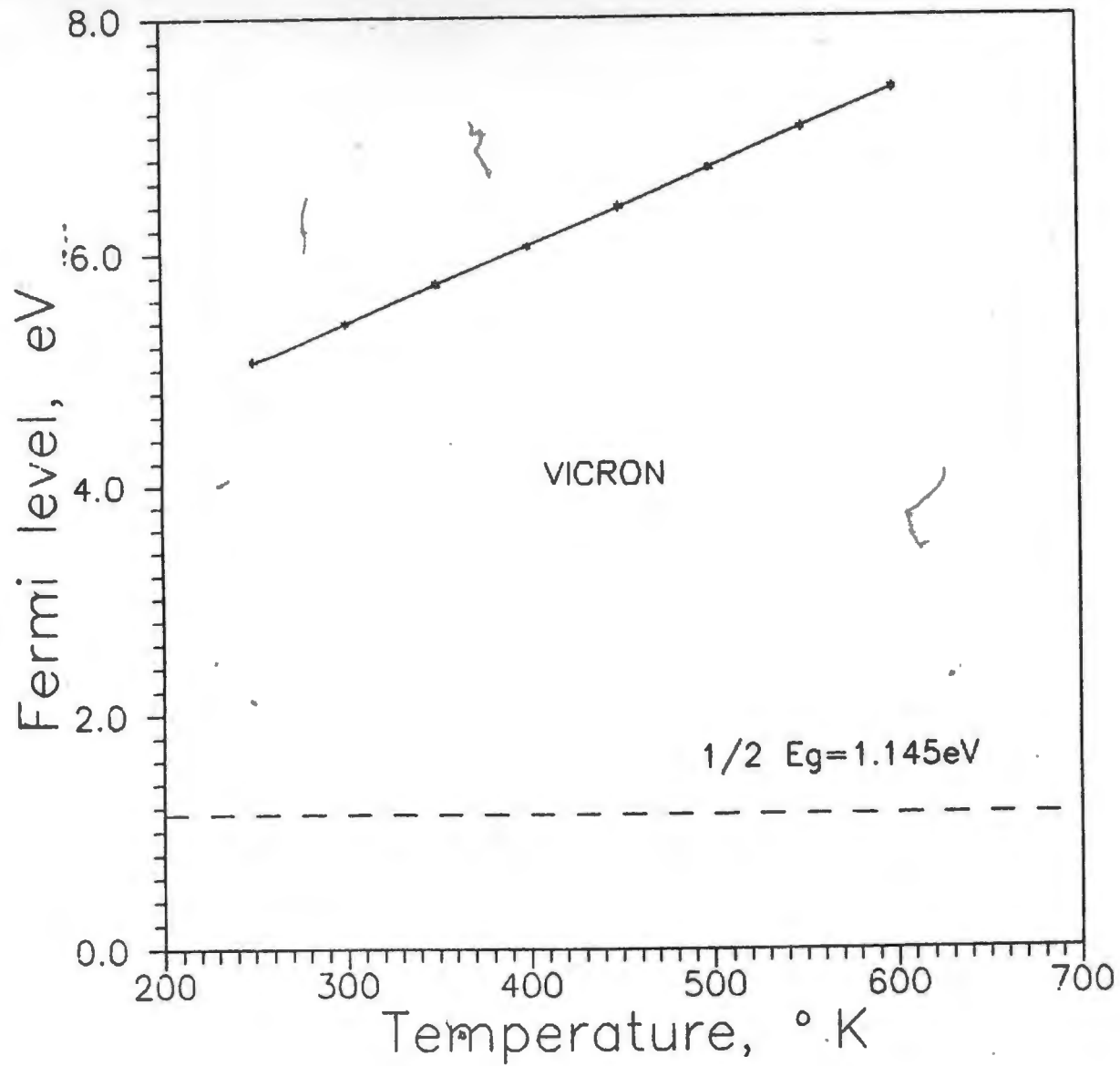
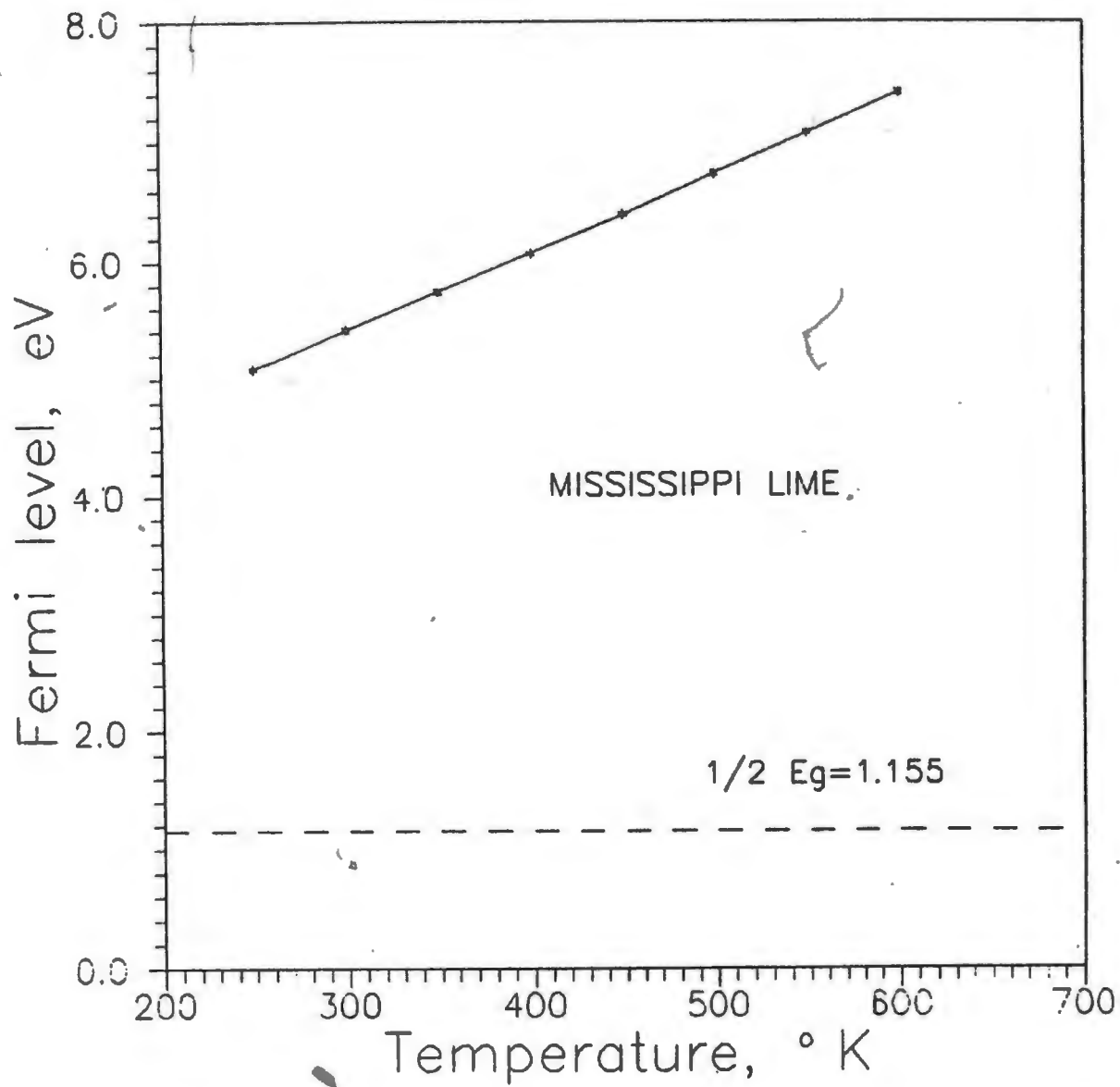


Figure 30. Position of Fermi level as a function of temperature for Mississippi lime.



SECTION VI

SUMMARY

1. Conductivity measurement figures show different shapes of the conductivity curves but the curves show the same trend at high temperatures. The E_g values ranged from 2.168 eV for Mississippi Lime, to 2.31 eV for Iceland spar. The values were very close to the 2.2 eV measured by Carta M. et al. who made similar measurements on calcite.
2. The variation of the charge carrier concentrations in relation to temperatures shows that the materials are all similar electrophysically because of the similar E_g values ranging from 1.17 cm^{-3} for Mississippi Lime, to $4.03 \times 10^{10} \text{ cm}^{-3}$ for Iceland spar.
3. From calculations the thermoelectric power values ranged from -7 eV to -11 eV. The values were then used for the determination of Fermi energy levels.
4. The calculated Fermi energy levels show all the materials, regardless of manner of sample preparation, to be "n" type semiconductors. The values of Fermi level ranged about from 4.9 eV to 7.8 eV as temperature is increased.

REFERENCES

1. Plaksia I. N. and Shafeev R. Sb. Osnovnye razdelenia mineralov, obladayouchchikh polyprovodkivom i svoiscualb electrostaticheskoy polozheniye. **INSTITUTE OF GEOL. Sci. Acad. Sci. USSR** (1966), 18p.
eachcation
2. Carta M. and Ciccu R. The influence of the surface energy structure of minerals and flotation. In 9th Int. Miner. Process. Congr., Prague, 1970 (Prague: Ustav Pro Vyzkhum Rud, 1970), vol. 1, 47-57.
3. Bragg and Nye, Proc. Roy. Soc. (London), A190, 1947, p. 474.
4. W. Kingery, H. Bowen, D. Uhlmann, Introduction to Ceramics(2nd Edition), John wiley & Sons, p.153.
5. H.S. Hanna and P. Somasundaran, Flotation of Salt-Type Minerals, Flotation, A.M. Gaudin Memorial Volume I, Society of Mining Engineers, 1976.

6. Hoberg H. Untersuchungen zur Deutung der Änderung der Flotierbarkeit halbleitender Erzminerale durch Bestrahlung im Kernreaktor. Aachener Blätter, 17, June 1967, 77p.

7. Carta M. et al. 8th Int. Miner. Process. Congr., Leningrad 1968, paper B-1, 12p.

8. Carta M. Revue Ind. Miner., 51, 1969, 480-97.

9. Ciccu R. and Foreman W. E. Sul Industria Min., 19, 1968, 525-31.

10. Revnivitsev V. I. et al. In 9th Int. Miner. Process. Congr., Prague 1970, vol. 1, 79-88.

11. Plaksin I. N. Shafeyev R. Su. and Chanturia V. A. 8th Int. Miner. Process. Congr., Leningrad 1968, paper S-3, 8p. ^

12. Plaksin I. N. In International mineral processing congress, 1960, 253-68; 390-2.

13. Tamm I. Z. Phys., 76, 1932 849-50; Phys.Z. 1932, 733-46; Chem. Abstr., 26, 1932, 5837

14. Shockley W. On the surface states associated with a periodic potential. Phys, Rev., 56, 1939, 317-23.
15. F. Fraas; Eletrostatic Separation of Granular Materials, Bulletin 603, U.S. Bureau of Mines, 1962.
16. F. Fraas; Mining Technology, AIME, 1947, vol 1. 11 p2257.
17. Rey M. and Formanek V. In Internationnal mineral processing congress, 1960(London: IMM, 1960), 343-53.
18. Myasnikov I. A. Bull. Acad. Sci. USSR, Phys. Ser., 21, 1957, 192-200.
19. Manca, P., A relation between the binding energy and the band gap energy in semi-conductors of diamond or zinc-blende structure - J. Phy. Chem. Solids - Vol 20 (1961), 268-273.
20. Kalston, O. C., Electrostatic separation of mixed granular solids - Elsevier (1961), and references cited therein.
21. O'Kane D.F. An investigation of ternary semiconducting compounds. Doctoral thesis, University of Michigan, 1962.

22. H. Lee and R.W. Smith "Effect of Shape and Surface Factors of Fine Calcite".

23. E. H. Greener, D. H. Whitmore, and M. E. Fine, J. Chem. Phys., 34, 1017 (1961).

24. H. J. Goldsmid, Application of Thermoelectricity, (Meyhuen and Co., Ltd., London, 1960)

25. E. H. Greener, D. H. Whitmore, and M. E. Fine, J. Chem. Phys., 34, 1017(1961).

26. R. F. Janninck, The Electrical Conductivity of Alpha-Nb₂O₅ and Nb₂O₄, Ph. D. thesis Northwestern University.

APPENDIX I
DISCUSSION OF INTRINSIC CONDUCTIVITY

The reason that the range in which σ and Q are independent of pressure is also the intrinsic range is seen as follows:

$$n_{\text{total}} = n_{\text{thermal}} + n_{\text{defects}}$$

where

n_{total} = the total number of electrons in the conduction band

n_{thermal} = the number of electrons in the conduction band due to the intrinsic activation process

n_{defects} = the number of electrons in the conduction band due to defect formation

Equation (6) has shown that

$$n_{\text{defects}} \propto P^{-1/a}$$

At constant temperature,

$$\sigma = q M (n_{\text{total}}) = q M (n_{\text{thermal}} + K P^{-1/a})$$

M is electron mobility

If the conductivity is not a function of pressure at constant temperature, then

$$n_{\text{total}} \approx n_{\text{thermal}}$$

This is the condition for intrinsic conductivity.

APPENDIX II
THERMOELECTRIC POWER

The thermoelectric power (Seebeck coefficient) Q is defined by the equation

$$Q = \lim_{\Delta T \rightarrow 0} V/\Delta T$$

where V is the terminal voltage and $\Delta T = T_1 - T_2$. The coefficient Q is temperature dependent and is a composite property of two materials. Since the electric fields set up by the temperature gradient act in the same direction and the thermoelectric power will be equal to the difference between the absolute thermoelectric powers of the individual materials

$$Q = Q_1 - Q_2$$

For finite temperature differences between the two materials, the terminal voltage and the thermoelectric power are related through

$$V = \int_{T_1}^{T_2} Q \, dT$$

APPENDIX III

DATA OF THERMOELECTRIC POWER AND FERMI LEVEL (ICELAND SPAR, ALBASPHERE, ALBACAR, ULTRAFINE, ALBAGLOS, VICROW, MISSISSIPPI LIME)

T=	250.0000	ES=	2.210000
EF =	4.831559	D=	-11.05243
T=	300.0000	EG=	2.210000
EF =	5.261547	D=	-10.33843
T=	350.0000	EE=	2.210000
EF =	5.592419	D=	-9.631525
T=	400.0000	EG=	2.210000
Ts	250.0000	EE=	2.249000
EF =	4.990025	D=	-11.13053
T=	300.0000	EE=	2.249000
EF =	5.320083	D=	-10.40851
T=	250.0000	EG=	2.249000
EF =	5.651154	D=	-9.887308
T=	400.0000	EG=	2.249000
EF =	5.982154	D=	-9.502474
T=	450.0000	EG=	2.249000
EF =	6.315965	D=	-9.204462
T=	500.0000	EG=	2.249000
EF =	6.649446	D=	-8.968391
T=	550.0000	EG=	2.249000
EF =	6.983675	D=	-8.74011
Ts	600.0000	EG=	2.249000
EF =	7.318444	D=	-8.616677

T=	300.0000	EG=	2.290000
EF =	5.381620	Q=	-16.47193
T=	350.0000	EG=	2.290000
EF =	5.712692	Q=	-9.945953
T=	400.0000	EG=	2.290000
EF =	6.044692	Q=	-9.553789
T=	450.0000	EG=	2.290000
EF =	6.377502	Q=	-9.270774
T=	500.0000	EG=	2.290000
EF =	6.711030	Q=	-9.009442
T=	550.0000	EG=	2.290000
EF =	7.045212	Q=	-8.813731
T=	600.0000	EG=	2.290000
EF =	7.379981	Q=	-8.650887

T=	250.0000	EG=	2.300000
EF =	5.066641	Q=	-11.23265
T=	300.0000	EG=	2.300000
EF =	5.396629	Q=	-10.48862
T=	350.0000	EG=	2.300000
EF =	5.727701	Q=	-9.960257
T=	400.0000	EG=	2.300000
EF =	6.059700	Q=	-9.566305
T=	450.0000	EG=	2.300000
EF =	6.392511	Q=	-9.261700
T=	500.0000	EG=	2.300000
EF =	6.726042	Q=	-9.019455
T=	550.0000	EG=	2.300000
EF =	7.060222	Q=	-8.822433
T=	600.0000	EG=	2.300000
EF =	7.394990	Q=	-8.659230
T=	250.0000	EG=	2.264000
EF =	5.012609	Q=	-11.16056
T=	300.0000	EG=	2.264000
EF =	5.342597	Q=	-10.42854
T=	350.0000	EG=	2.264000
EF =	5.673668	Q=	-9.905764

Ts	450.0000	ES:	2.244000
EF	4.305444	D:	-9.521249
T=	450.0000	ES:	2.244000
EF	4.338478	O:	-9.221450
T+	500.0000	EC:	2.244000
EF	4.472000	O:	-8.983410
T*	550.0000	EC:	2.244000
EF	7.006000	O:	-8.789445
T=	400.0000	EC:	2.244000
EF	7.340058	O:	-8.429193
T=	250.0000	EC:	2.220000
EF	5.021414	O:	-11.17258
T=	300.0000	EC:	2.270000
EF	5.351402	O:	-10.43855
T=	350.0000	EC:	2.270000
EF	5.482473	O:	-9.917344
T=	400.0000	EC:	2.270000
EF	4.014473	O:	-9.526758
T=	450.0000	EC:	2.270000
EF	4.347484	O:	-9.228325
T*	500.0000	EC:	2.270000
EF	4.481014	O:	-8.989417
T=	550.0000	EC:	2.270000
EF	7.015904	O:	-8.795127
T=	400.5300	EC:	2.270000
EF	7.249943	O:	-8.434199
T=	250.0000	EC:	2.310000
EF	5.071451	R:	-11.25248
T+	300.0000	EC:	2.310000
EF	5.401438	O:	-10.50530
T*	350.0000	EC:	2.310000
EF	5.742710	O:	-9.974541
T=	400.0000	EC:	2.315000
EF	4.074710	P:	-4.57121
T=	450.0000	EC:	2.310000
EF	4.407520	C:	-0.272324
T*	500.0000	EC:	2.310000
EF	4.741051	O:	-9.02448
T+	550.0000	EC:	2.310000
EF	7.075231	P:	-8.831534